



Synthesis, solvent interactions and computational study of monocarbohydrazones

Gorana S. Mrdjan¹ · Borko M. Matijević¹ · Gyöngyi Gy. Vastag¹ · Aleksandra R. Božić² · Aleksandar D. Marinković³ · Miloš K. Milčić⁴ · Ivana N. Stojiljković⁵

Received: 27 September 2019 / Accepted: 14 February 2020 / Published online: 21 February 2020
© Institute of Chemistry, Slovak Academy of Sciences 2020

Abstract

Carbohydrazones are compounds that are increasingly studied due to their wide potential biological activity. Monocarbohydrazones (mCHs), as one of the carbohydrazone derivatives, so far have been poorly investigated. For a more detailed study, in this paper, eighteen compounds of monocarbohydrazones (eight known and ten newly synthesized derivatives) were synthesized and characterized using NMR and IR spectroscopy. As carbohydrazones show *E/Z* isomerization caused by the presence of the imino group, some of the synthesized mCHs are in the form of a mixture of these two isomers. The effects of specific and nonspecific solvent–solute interactions on the UV absorption maxima shifts were evaluated using linear free energy relationships principles, i.e., using Kamlet–Taft’s and Catalan’s models. For more information about interactions between dissolved substance and the surrounding medium, correlations have been made with Hansen’s solubility parameters. The influence of the structure on the spectral behavior of the compounds tested was interpreted using Hammett’s equation. Experimentally obtained physicochemical properties of mCHs were compared to and confirmed with computational methods that included TD-DFT calculations and MP2 geometry optimizations.

Electronic supplementary material The online version of this article (<https://doi.org/10.1007/s11696-020-01106-4>) contains supplementary material, which is available to authorized users.

✉ Gorana S. Mrdjan
gorana.mrdjan@dh.uns.ac.rs

¹ Department of Chemistry, Biochemistry and Environmental Protection, Faculty of Sciences, University of Novi Sad, Trg Dositeja Obradovića 3, Novi Sad 21000, Serbia

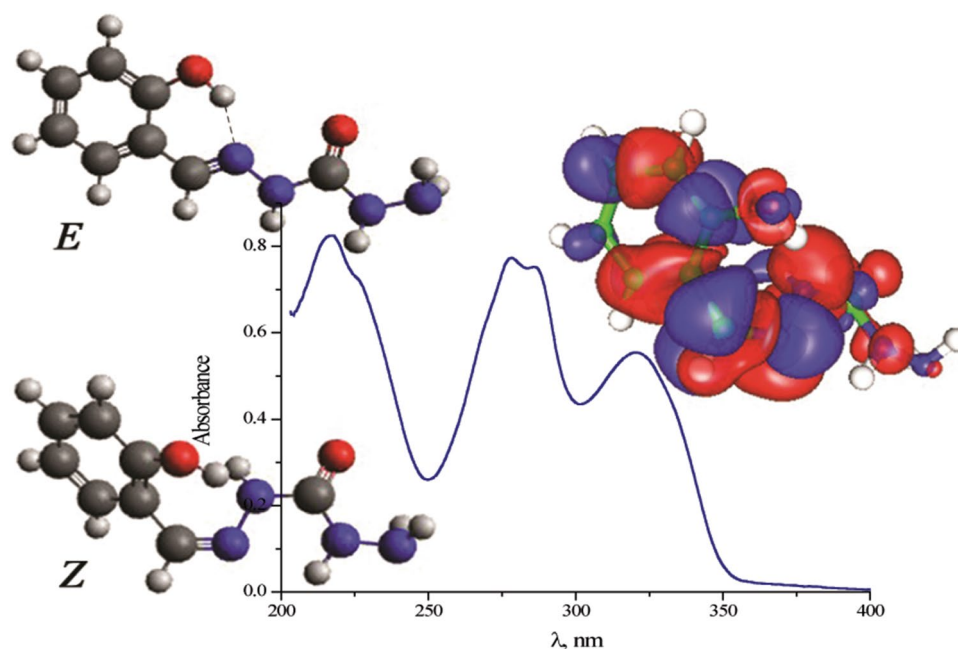
² Belgrade Polytechnic, Brankova 17, Belgrade 11000, Serbia

³ Faculty of Technology and Metallurgy, University of Belgrade, Karnegijeva 4, Belgrade 11000, Serbia

⁴ Faculty of Chemistry, University of Belgrade, Studentski trg 12-16, Belgrade 11000, Serbia

⁵ Faculty of Forestry, University of Belgrade, Kneza Visaslava 1, Belgrade 11000, Serbia

Graphic abstract



Keywords Monocarbohydrazones · Solvent interactions · Substituent effects · Molecular geometry optimization · TDF calculations

Introduction

Carbohydrazone represents a hydrazine derivative of carbonic acid that possesses two reactive hydrazine groups capable of condensation with one or two carbonyl compounds to produce mono- and bis-carbohydrazones, respectively (Zhang et al. 2006). Due to the wide biological and clinical activity, this group of compounds is becoming an area of great interest to scientists. Previous studies have shown that they possess anticancer, anti-tumor, antioxidant, anti-viral, anti-inflammatory, antimicrobial and anti-diabetic activity (Bacchi et al. 1999; Rollas and Küçükgül 2007; Gangarapu et al. 2014; Kajal et al. 2014; Božić et al. 2016; Božić et al. 2017a). In addition to the biological activity, carbohydrazones have also proved to be good oxygen reduction catalysts (Kamyabi et al. 2017) and carbonic anhydrase inhibitors (Iqbal et al. 2017). Also, for example, the most structurally characterized monocarbohydrazones (mCHs)—salicylaldehydecarbohydrazone—are known as an aluminum detector in water (Sánchez Rojas et al. 1994). Furthermore, due to their reactivity, they can easily react with various transition metals and build complexes (Babahan et al. 2011; Shebl and Khalil 2015; Draganca et al. 2016; Gholivand et al. 2016; Wang et al. 2017). Some of the complexes made with Cd(II), for example, show better antimicrobial activity than the ligands themselves (Montazerzohori et al. 2014).

Considering their wide application, mCHs have been slightly tested and all reports lack detailed structural and theoretical study. Because of that, in this work, we report the synthesis and characterization of eighteen mCHs, of which eight are already known and ten are newly synthesized. All compounds were characterized using NMR, IR, UV–Vis spectroscopy and elemental analysis. Previous studies have shown that carbohydrazones might exist in keto or enol tautomeric form and adopt *E* or *Z* configuration around the imino group (Zelenin et al. 1999). In this work, some of the synthesized compounds were presented as a mixture of both isomers, and their stereochemistry was proven with the use of 2D homonuclear (NOESY) and heteronuclear (HSQC and HMBC) NMR techniques.

The UV data were analyzed using LSER and LFER models, respectively, to evaluate the influence of solvent/solute interactions and substituent effects on the spectra of the investigated compounds. The effect of solvent was interpreted by two most commonly used models, Catalan's and Kamlet–Taft's. Also, for additional information on the interactions between the solvent and the dissolved substance, correlations with Hansen's solubility parameters have been made. The influence of the type of substituent, as well as their position, on the benzene ring was characterized by Hammett's equation. Experimentally obtained physicochemical properties of monocarbohydrazones were

compared to and confirmed with computational methods that included TD-DFT calculations and MP2 geometry optimizations. Charge-transfer distance (DCT), amount of transferred charge (QCT) and Tozer's Λ diagnostic index were evaluated according to the method proposed by Le Bahers. Orbitals with the highest contribution to the nature of the first excited state were localized with the NBO localization procedure.

Experimental

Materials

All chemicals used for synthesis were from Sigma-Aldrich and with the quality of the synthesis. They were used without prior purification. Solvents used for recording the UV spectra were also from Sigma-Aldrich and with high degree of purity and quality for spectrophotometric measurements: methanol, ethanol, *n*-propanol, *n*-butanol, *n*-pentanol, *i*-propanol, *i*-butanol, *t*-butanol, acetic acid, acetonitrile (AcN), dimethyl sulfoxide (DMSO), *N,N*-dimethylformamide (DMF), dichloromethane (DCM), chloroform, ethyl acetate (EtAc), tetrahydrofuran (THF), 1,4-dioxane and diethyl ether.

Melting points of tested compounds were determined with Kofler's device. The elemental analysis was performed using a Vario El III elemental analyzer. IR spectra were recorded on a Nicolet Nexus 670 FTIR (Thermo Scientific) spectrophotometer, in the range of 400–4000 cm^{-1} using the KBr pellet technique. NMR spectral assignments and structural parameters were obtained by the combined use of 1D (^1H and ^{13}C) and 2D (NOESY, ^1H - ^{13}C HSQC and ^1H - ^{13}C HMBC) spectroscopy. The NMR spectra were performed on Bruker Avance 400 equipped with a broadband direct probe. Chemical shifts are given on δ scale relative to tetramethylsilane (TMS) as an internal standard for ^1H and ^{13}C . Coupling constants (J) were expressed in Hz. Abbreviations used for NMR spectra are: s, singlet; dd, doublet of doublets; t, triplet; m, multiplet. UV absorption spectra were recorded by using a Shimadzu UV-1800 spectrophotometer in 1.00-cm cells at 25 ± 0.1 °C at concentration of 4×10^{-5} mol dm^{-3} .

Geometries of *Z* and *E* isomers of all investigated molecules were optimized in gas phase by the MP2 method using the 6-311G(*d,p*) basis set. To find the global minimum on the potential energy surface, multiple geometry optimizations were performed for every compound starting from different initial geometries and minimizing the energy concerning all geometrical parameters. The nature of the lowest energy minimum was further confirmed with frequency calculations; no negative frequencies were found.

In order to estimate a nature of excitations [charge-transfer (CT) or local excitations (LE)], Tozer's Λ diagnostic index (Peach et al. 2008) was calculated for all the

investigated compounds with time-dependant (TD) density functional theory (DFT) method using long-range corrected CAM-B3LYP functional (Yanai et al. 2004) and 6-311G(*d,p*) basis set in gas phase. The nature of investigated excitations was further confirmed by calculating qualitative charge-transfer indices including the charge-transfer distance (D_{CT}) and amount of transferred charge (Q_{CT}). The ground-state (DFT) and excited-state (TD-DFT) electron densities were calculated at MP2/6-311G(*d,p*) optimized geometries with the CAM-B3LYP/6-311G(*d,p*) functional/basis set. The charge-transfer indices were calculated from obtained ground- and excited-state electron densities according to the method proposed by Le Bahers et al. (2011) with CT program (Jacquemin et al. 2012).

Theoretical absorption spectra are calculated starting from MP2/6-311G(*d,p*) optimized geometries in two different solvents: DMSO and methanol with the TD-DFT method. These TD-DFT calculations were done with B3LYP functional (Becke 1993) and 6-311G(*d,p*) basis set. Solvent effects have been simulated with the standard static isodensity surface-polarized continuum model (IPCM) (Wiggins et al. 2009).

In order to visualize the nature of the first excited state, the orbitals with the highest contribution to this excited state were localized with NBO localization procedure (Reed and Weinhold 1985) using the NBO 3.1 program (Glendening et al. 2003).

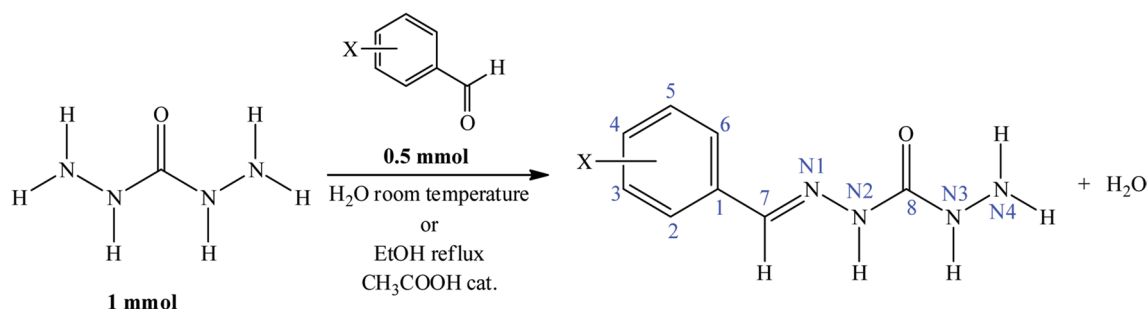
All quantum chemical calculations were carried out using the Gaussian 09 program (Frisch et al. 2016).

Synthesis and results of characterization of *N*-benzylidene-carbohydrazones

The basic compound for the synthesis of mCHs, carbohydrazide (dhO), was prepared according to a well-known procedure (Zhang et al. 2006). The purity of the synthesized dhO was checked by NMR spectroscopy, elemental analysis and melting point (M.p. 153 °C, M.p. Lit. data 153–154 °C) (Kurzer and Wilkinson 1970).

Monocarbohydrazones (**1–18**) were synthesized by the reaction between dhO (1 mmol) and appropriate benzaldehydes (0.5 mmol) in two different solvents, depending on the aggregate state of aldehydes that were added. The general procedure for the synthesis of mCHS is shown in Scheme 1.

Compounds **3**, **4**, **8–11**, **15** and **17** were obtained by reaction of the carbohydrazide dissolved in ethanol [30 ml, (70%)] and the corresponding benzaldehyde also dissolved in ethanol (10 ml). The reaction was carried out under reflux for 2.5 h. A drop of glacial acetic acid was added as a catalyst at the beginning of the reaction. Compounds **1**, **2**, **5–7**, **12–14**, **16** and **18** were prepared in an analogous manner (molar ratio) applied within the previously shown procedure, using water as a dissolving solvent (10 ml) at room



Compound	Reactant (X)
1	H
2/3/4	<i>o/m/p</i> - OH
5/6/7	<i>o/m/p</i> - CH ₃
8/9/10	<i>o/m/p</i> - NO ₂
11/12/13	<i>o/m/p</i> - OCH ₃
14/15	<i>m/p</i> - Cl
16/17	<i>m/p</i> - Br
18	<i>p</i> - F

Scheme 1 Reaction of synthesis of monocarbohydrazones

temperature with one drop of glacial acetic acid. The reaction mixture was stirred for 0.5 h. After synthesis, all compounds were collected by filtration and washed successively with cold alcohol and diethyl ether, dried and recrystallized from a suitable solvent. Compounds **1** and **2** (Božić et al. 2017b), **4** and **13** (Okawara et al. 2006), **7**, **15** and **18** (Warkentin et al. 1977) and **10** (Zelenin et al. 1999) are known compounds that have been previously synthesized. All these compounds are synthesized by our procedures, and their purity was verified through melting point, elemental analysis, IR and NMR spectroscopy. Compounds **7**, **15** and **18** are known, but they are not characterized. Obtained results for substances **1**, **2**, **4**, **10** and **13** are in agreement with the literature data. A list of synthesized compounds with numeration of the atoms of interest is given in Scheme 1.

Benzaldehydecarbohydrazone (**1**)

White substance, recrystallized from ethanol. Yield: 81%. m.p. 172–174 °C (literary m.p. 173 °C). Elemental analysis: calculated for C₈H₁₀N₄O (Mw=178.37 g mol⁻¹): C, 53.92; H, 5.66; N, 31.44; O, 8.98%. Found: C, 53.81; H, 5.02; N, 30.87; O, 10.30%. IR (KBr, cm⁻¹) ν_{\max} : 3319 m (NH₂), 3092w (NH), 1682 s (C=O), 1601 m (C=N), 1551 s and 1448 m (C=Carom.), 753 m and 697 m (C–H band (mono)). ¹H NMR (400 MHz, DMSO-*d*₆, δ (ppm)): 4.05 (s, 2H, H₂–N₄), 7.73 (d, 2H, H–C₂=H–C₆, ³J_{2,3}=6.9 Hz = ³J_{6,5}=6.9 Hz), 7.32–7.40 (m, 3H, H–C₃, H–C₄, H–C₅), 7.87 (s, 1H, H–N₃), 8.01 (s, 1H, H–C₇), 10.38 (s, 1H, H–N₂). ¹³C NMR (126 MHz, DMSO-*d*₆, δ (ppm)): 127.13 (C₃=C₅); 129.03 (C₂=C₆); 129.57 (C₄); 135.13 (C₁); 140.82 (C₇);

157.59 (C₈). Lit. data: ¹H NMR (100 MHz, DMSO-*d*₆, δ (ppm)): 4.10 (s, 2H, H₂–N₄), 7.2–7.5 (m, 2H, H–C₂, H–C₆), 7.60–7.80 (m, 3H, H–C₃, H–C₄, H–C₅), 7.92 (s, 1H, H–N₃), 8.10 (s, 1H, H–C₇), 10.50 (s, 1H, H–N₂). ¹³C NMR (126 MHz, DMSO-*d*₆, δ (ppm)): 125.49 (C₃=C₅); 128.68 (C₂=C₆); 131.61 (C₄); 134.85 (C₁); 140.76 (C₇); 157.20 (C₈) (Božić et al. 2017b).

2-Hydroxybenzaldehyde carbohydrazone (**2**)

White substance, recrystallized from ethanol. Yield: 76%. m.p. 191 °C. Elemental analysis: Calculated for C₈H₁₁N₄O₂ (Mw=194.37 g mol⁻¹): C, 49.48; H, 5.19; N, 28.85; O, 16.48%. Found: C, 49.11; H, 5.12; N, 28.78; O, 16.99%. IR (KBr, cm⁻¹) ν_{\max} : 3353 (OH), 3283 s (NH₂), 3098 m (NH), 1681 s (C=O), 1633 m (C=N), 1556 s and 1491 m (C=Carom.), 1169 m-s (Ar–OH); 739 m (C–H band (*ortho*)). ¹H NMR (400 MHz, DMSO-*d*₆, δ (ppm)): 4.16 (s, 2H, H₂–N₄), 6.79–6.89 (m, 2H, H–C₅, H–C₃), 7.18 (td, 1H, H–C₄, ³J_{4,5}=7.7 Hz, ⁴J_{4,6}=1.4 Hz), 7.64 (s, 1H, H–C₆), 7.92 (s, 1H, H–N₃), 8.22 (s, 1H, H–C₇), 10.08–10.73 (spm, 2H, OH, H–N₂). ¹³C NMR (126 MHz, DMSO-*d*₆, δ (ppm)): 116.09 (C₆), 119.22 (C₄), 120.06 (C₁), 127.86 (C₃), 130.23 (C₅), 140.22 (C₇), 156.24 (C₂), 157.92 (C₈). Lit. data: ¹H NMR (500 MHz, DMSO-*d*₆, δ (ppm)): 4.16 (s, 2H, H₂–N₄), 6.79–6.89 (m, 2H, H–C₅, H–C₃), 7.18 (td, 1H, H–C₄, ³J_{4,5}=7.7 Hz, ⁴J_{4,6}=1.4 Hz), 7.64 (s, 1H, H–C₆), 7.92 (s, 1H, H–N₃), 8.22 (s, 1H, H–C₇), 10.08–10.73 (spm, 2H, OH, H–N₂). ¹³C NMR (126 MHz, DMSO-*d*₆, δ (ppm)): 116.09 (C₆), 119.22 (C₄), 120.06 (C₁), 127.86 (C₃), 130.23 (C₅), 140.22 (C₇), 156.24 (C₂), 157.92 (C₈) (Božić et al. 2017b).

3-Hydroxybenzaldehyde carbohydrazone (3)

Yellow substance, recrystallized from ethanol. Yield: 58%. m.p. 148 °C. Elemental analysis: Calculated for $C_8H_{11}N_4O_2$ (Mw = 194.37 $gmol^{-1}$): C, 49.48; H, 5.19; N, 28.85; O, 16.48%. Found: C, 48.96; H, 5.03; N, 28.66; O, 17.35%. IR (KBr, cm^{-1}) ν_{max} : 3337 m (OH), 3304 s (NH_2), 3091 m (NH), 1669 s (C=O), 1617 m (C=N), 1529 s and 1454 m (C=C arom.), 1270 m-s (Ar-OH), 781 s and 686 s (C-H band (*meta*)). **Ratio E:Z isomers (86:14). Isomer E:** 1H NMR (400 MHz, DMSO- d_6 , δ (ppm)): 4.07 (s, 2H, H2-N4), 6.76 (d, 1H, H-C4, $^3J_{4,5} = 7.6$ Hz), 7.11–7.23 (m, 3H, H-C2, H-C5, H-C6), 7.78 (s, 1H, H-N3), 7.90 (s, 1H, H-C7), 9.51 (s, 1H, H-OH), 10.34 (s, 1H, H-N2). ^{13}C NMR (126 MHz, DMSO- d_6 , δ (ppm)): 113.43 (C2), 116.80 (C4), 118.34 (C6), 130.01 (C5), 136.38 (C1), 141.04 (C7), 157.54 (C3), 157.97 (C8). **Isomer Z:** 1H NMR (400 MHz, DMSO- d_6 , δ (ppm)): 4.07 (s, 2H, H2-N4), 6.80 (d, 1H, H-C4, $^3J_{4,5} = 7.9$ Hz), 7.11–7.23 (m, 3H, H-C2, H-C5, H-C6), 7.82 (s, 1H, H-N3), 8.09 (s, 1H, H-C7), 9.58 (s, 1H, H-OH), 10.63 (s, 1H, H-N2). ^{13}C NMR (126 MHz, DMSO- d_6 , δ (ppm)): 113.54 (C2), 117.16 (C4), 118.63 (C6), 130.12 (C5), 136.46 (C1), 152.53 (C7), 158.06 (C3), 162.47 (C8).

4-Hydroxybenzaldehyde carbohydrazone (4)

White substance, recrystallized from methanol. Yield: 69%. m.p. 223–225 °C. Elemental analysis: Calculated for $C_8H_{11}N_4O_2$ (Mw = 194.37 $gmol^{-1}$): C, 49.48; H, 5.19; N, 28.85; O, 16.48%. Found: C, 49.27; H, 5.22; N, 28.89; O, 16.62%. IR (KBr, cm^{-1}) ν_{max} : 3430 m (OH), 3318 s (NH_2), 3069 m (NH), 1698 s (C=O), 1637 m (C=N), 1518 s and 1442 m (C=Carom.), 1241 m-s (Ar-OH); 824 m (C-H band (*para*)). 1H NMR (400 MHz, DMSO- d_6 , δ (ppm)): 4.06 (s, 2H, H2-N4), 6.76 (d, 2H, H-C5=H-C3 $^3J_{3,2} = ^3J_{5,6} = 8.6$ Hz), 7.55 (d, 2H, H-C6=H-C2, $^3J_{2,3} = ^3J_{6,5} = 8.6$ Hz), 7.75 (s, 1H, H-C7), 7.85 (s, 1H, H-N3), 9.77 (s, 1H, OH), 10.16 (s, 1H, H-N2). ^{13}C NMR (126 MHz, DMSO- d_6 , δ (ppm)): 115.88 (C3=C5), 126.26 (C1), 128.76 (C2=C6), 141.00 (C7), 157.75 (C8), 158.98 (C4). Lit. data: 1H NMR (500 MHz, DMSO- d_6 , δ (ppm)): 4.04 (s, 2H, H2-N4), 6.74 (d, 2H, H-C5, H-C3), 7.53 (d, 2H, H-C6, H-C2), 7.73 (s, 1H, H-C7). ^{13}C NMR (126 MHz, DMSO- d_6 , δ (ppm)): 115.00 (C3=C5), 125.00 (C1), 128.00 (C2=C6), 140.00 (C7), 157.00 (C8), 158.22 (C4) (Okawara et al. 2006).

2-Methylbenzaldehyde carbohydrazone (5)

White substance, recrystallized from *n*-propanol. Yield: 61%. m.p. > 240 °C. Elemental analysis: Calculated for $C_9H_{12}N_4O$ (Mw = 192.38 $gmol^{-1}$): C, 56.24; H, 6.29; N, 29.15; O, 8.32%. Found: C, 55.71; H, 6.37; N, 29.01; O,

8.73%. IR (KBr, cm^{-1}) ν_{max} : 3297 m (NH_2), 3090 m (NH), 1678 s (C=O), 1645 m (C=N), 1522 s and 1458 m (C=C arom.), 751 m (C-H band (*ortho*)). 1H NMR (400 MHz, DMSO- d_6 , δ (ppm)): 2.36 (s, 3H, CH3), 4.09 (s, 2H, H2-N4), 7.16–7.29 (m, 3H, H-C5, H-C4, H-C3), 7.90 (s, 1H, H-C7), 7.96 (d, 1H, H-C6, $^3J_{6,5} = 7.3$ Hz), 8.16 (s, 1H, H-N3), 10.30 (s, 1H, H-N2). ^{13}C NMR (126 MHz, DMSO- d_6 , δ (ppm)): 19.43 (CH3), 126.22 (C6), 126.44 (C1), 129.27 (C3), 131.04 (C4), 133.03 (C6), 136.26 (C2), 139.27 (C7), 157.52 (C8).

3-Methylbenzaldehyde carbohydrazone (6)

White substance, recrystallized from ethanol. Yield: 63%. m.p. 179–181 °C. Elemental analysis: Calculated for $C_9H_{12}N_4O$ (Mw = 192.38 $gmol^{-1}$): C, 56.24; H, 6.29; N, 29.15; O, 8.32%. Found: C, 55.91; H, 6.42; N, 29.33; O, 8.34%. IR (KBr, cm^{-1}) ν_{max} : 3304 s (NH_2), 3083 m (NH), 1676 s (C=O), 1614 m (C=N), 1521 s (C=Carom.), 788 s and 692 s (C-H band (*meta*)). 1H NMR (400 MHz, DMSO- d_6 , δ (ppm)): 2.32 (s, 3H, CH3), 4.08 (s, 2H, H2-N4), 7.15 (d, 1H, H-C4, $^3J_{4,5} = 7.6$ Hz), 7.26 (t, 1H, H-C5, $^3J_{5,4} = 7.6$ Hz), 7.48 (d, 1H, H-C6, $^3J_{6,5} = 7.6$ Hz), 7.60 (s, 1H, H-C2), 7.82 (s, 1H, H-C7), 8.00 (s, 1H, H-N3), 10.36 (s, 1H, H-N2). ^{13}C NMR (126 MHz, DMSO- d_6 , δ (ppm)): 21.33 (CH3), 124.59 (C6), 127.39 (C5), 128.89 (C2), 130.22 (C4), 135.12 (C1), 138.22 (C3), 140.66 (C7), 157.57 (C8).

4-Methylbenzaldehyde carbohydrazone (7)

White substance, recrystallized from methanol. Yield: 67%. m.p. 225–228 °C. Elemental analysis: Calculated for $C_9H_{12}N_4O$ (Mw = 192.38 $gmol^{-1}$): C, 56.24; H, 6.29; N, 29.15; O, 8.32%. Found: C, 56.39; H, 6.17; N, 29.12; O, 8.32%. IR (KBr, cm^{-1}) ν_{max} : 3341 m (NH_2), 3079 m (NH), 1668 s (C=O), 1610 m (C=N), 1509 s and 1480 m (C=C arom.), 830 m (C-H band (*para*)). 1H NMR (400 MHz, DMSO- d_6 , δ (ppm)): 2.31 (s, 3H, CH3), 4.10 (s, 2H, H2-N4), 7.19 (d, 2H, H-C5=H-C3 $^3J_{3,2} = ^3J_{5,6} = 7.9$ Hz), 7.62 (d, 2H, H-C6=H-C2, $^3J_{2,3} = ^3J_{6,5} = 7.9$ Hz), 7.82 (s, 1H, H-C7), 7.98 (s, 1H, H-N3), 10.33 (s, 1H, H-N2). ^{13}C NMR (126 MHz, DMSO- d_6 , δ (ppm)): 21.41 (CH3), 127.10 (C3=C5), 129.62 (C2=C6), 132.51 (C1), 139.13 (C4), 140.74 (C7), 157.61 (C8) (Warkentin et al. 1977).

2-Nitrobenzaldehyde carbohydrazone (8)

Yellow substance, recrystallized from methanol. Yield: 72%. m.p. 237 °C. Elemental analysis: Calculated for $C_8H_9N_5O_3$ (Mw = 223.44 $gmol^{-1}$): C, 43.05; H, 4.06; N, 31.38; O, 21.50%. Found: C, 42.87; H, 4.12; N, 30.97; O, 22.04%. IR (KBr, cm^{-1}) ν_{max} : 3361 m (NH_2), 3088 m (NH), 1701 s (C=O), 1615 m (C=N), 1528 s and 1344 s (NO), 1593 m

and 1441 m (C=C arom.), 739 m (C–H band (*ortho*)). ^1H NMR (400 MHz, DMSO- d_6 , δ (ppm)): 4.14 (s, 2H, H2–N4), 7.57 (t, 1H, H–C4, $^3J_{4,3} = ^3J_{4,5} = 7.7$ Hz), 7.71 (t, 1H, H–C5, $^3J_{5,4} = ^3J_{5,6} = 7.7$ Hz), 7.98 (d, 1H, H–C3, $^3J_{3,4} = 7.7$ Hz), 8.16 (s, 1H, H–C7), 8.26 (s, 1H, H–N3), 8.41 (d, 1H, H–C6, $^3J_{6,5} = 7.7$ Hz), 10.78 (s, 1H, H–N2). ^{13}C NMR (126 MHz, DMSO- d_6 , δ (ppm)): 124.75 (C3), 128.53 (C1), 129.24 (C6), 131.06 (C4), 133.65 (C5), 135.30 (C7), 148.24 (C2), 157.18 (C8).

3-Nitrobenzaldehyde carbohydrazone (9)

Yellow substance, recrystallized from ethanol. Yield: 61%. m.p. 235 °C. Elemental analysis: Calculated for $\text{C}_8\text{H}_9\text{N}_5\text{O}_3$ (Mw = 223.44 g mol $^{-1}$): C, 43.05; H, 4.06; N, 31.38; O, 21.50%. Found: C, 43.14; H, 4.17; N, 31.37; O, 21.32%. IR (KBr, cm $^{-1}$) ν_{max} : 3327 m (NH $_2$), 3095 m (NH), 1718 s (C=O), 1616 m (C=N), 1530 s and 1354 s (NO), 1479 m (C=C arom.), 737 m and 674 m (C–H band (*meta*)). ^1H NMR (400 MHz, DMSO- d_6 , δ (ppm)): 4.10 (s, 2H, H2–N4), 7.66 (t, 1H, H–C5, $^3J_{5,6} = ^3J_{5,4} = 8.0$ Hz), 7.96 (s, 1H, H–C7), 8.16 (dd, 2H, H–C4=H–C6, $^3J_{6,5} = ^3J_{4,5} = 8.0$ Hz), 8.37 (s, 1H, H–C2), 8.62 (s, 1H, H–N3), 10.62 (s, 1H, H–N2). ^{13}C NMR (126 MHz, DMSO- d_6 , δ (ppm)): 121.20 (C2), 123.65 (C4), 130.48 (C5), 133.42 (C6), 137.24 (C1), 138.18 (C7), 148.85 (C3), 157.33 (C8).

4-Nitrobenzaldehyde carbohydrazone (10)

Yellow substance, recrystallized from ethanol. Yield: 66%. m.p. 220 °C. Elemental analysis: Calculated for $\text{C}_8\text{H}_9\text{N}_5\text{O}_3$ (Mw = 223.44 g mol $^{-1}$): C, 43.05; H, 4.06; N, 31.38; O, 21.50%. Found: C, 43.21; H, 4.12; N, 31.44; O, 21.23%. IR (KBr, cm $^{-1}$) ν_{max} : 3329 m (NH $_2$), 3084 m (NH), 1682 s (C=O), 1615 m (C=N), 1507 s and 1340 s (NO), 1526 m (C=C arom.), 844 m (C–H band (*para*)). **Ratio E:Z isomers (77:23).** **Isomer E:** ^1H NMR (400 MHz, DMSO- d_6 , δ (ppm)): 4.15 (s, 2H, H2–N4), 7.94 (s, 1H, H–C7), 8.02 (d, 2H, H–C5=H–C3 $^3J_{3,2} = ^3J_{5,6} = 8.4$ Hz), 8.19 (d, 2H, H–C6=H–C2, $^3J_{2,3} = ^3J_{6,5} = 8.4$ Hz), 8.32 (s, 1H, H–N3), 10.76 (s, 1H, H–N2). ^{13}C NMR (126 MHz, DMSO- d_6 , δ (ppm)): 124.19 (C2=C6), 127.93 (C3=C5), 138.12 (C1), 141.75 (C4), 147.99 (C7), 157.20 (C8). **Isomer Z:** ^1H NMR (400 MHz, DMSO- d_6 , δ (ppm)): 4.15 (s, 2H, H2–N4), 7.94 (s, 1H, H–C7), 8.02 (d, 2H, H–C5=H–C3 $^3J_{3,2} = ^3J_{5,6} = 8.4$ Hz), 8.27 (d, 2H, H–C6=H–C2, $^3J_{2,3} = ^3J_{6,5} = 8.4$ Hz), 8.32 (s, 1H, H–N3), 11.21 (s, 1H, H–N2). ^{13}C NMR (126 MHz, DMSO- d_6 , δ (ppm)): 124.37 (C2=C6), 128.15 (C3=C5), 141.36 (C4), 148.03 (C7), 152.23 (C8). Lit. data: **E:Z isomers (21:79)** **Isomer E:** ^1H NMR (400 MHz, DMSO- d_6 , δ (ppm)): 4.10 (s, 2H, H2–N4), 7.90 (s, 1H, H–C7), 8.01 (d, 2H, H–C5=H–C3 $^3J_{3,2} = ^3J_{5,6} = 8.4$ Hz), 8.21 (d, 2H,

H–C6=H–C2, $^3J_{2,3} = ^3J_{6,5} = 8.4$ Hz), 8.40 (s, 1H, H–N3), 10.80 (s, 1H, H–N2). **Isomer Z:** ^1H NMR (400 MHz, DMSO- d_6 , δ (ppm)): 4.10 (s, 2H, H2–N4), 7.38 (s, 1H, H–C7), 8.01 (d, 2H, H–C5=H–C3 $^3J_{3,2} = ^3J_{5,6} = 8.4$ Hz), 8.21 (d, 2H, H–C6=H–C2, $^3J_{2,3} = ^3J_{6,5} = 8.4$ Hz), 8.30 (s, 1H, H–N3), 11.30 (s, 1H, H–N2) (Zelenin et al. 1999).

2-Methoxybenzaldehyde carbohydrazone (11)

White substance, recrystallized from ethanol. Yield: 77%. m.p. 194 °C. Elemental analysis: Calculated for $\text{C}_9\text{H}_{12}\text{N}_4\text{O}_2$ (Mw = 208.38 g mol $^{-1}$): C, 58.81; H, 5.92; N, 27.43; O, 7.83%. Found: C, 58.33; H, 5.99; N, 27.48; O, 8.20%. IR (KBr, cm $^{-1}$) ν_{max} : 3300 m (NH $_2$), 3091 m (NH), 2998 m, 2841 m and 1465 m (O–CH $_3$), 1681 s (C=O), 1636 m (C=N), 1522 s and 1481 m (C=C arom.), 754 m (C–H band (*ortho*)). ^1H NMR (400 MHz, DMSO- d_6 , δ (ppm)): 3.82 (d, $J = 8.9$ Hz, 3H), 4.07 (s, 2H, H2–N4), 6.91–6.97 (m, 1H, H–C5), 7.03 (t, 1H, H–C3, $^3J_{3,4} = 8.2$ Hz), 7.26–7.41 (m, 1H, H–C4), 7.90–8.02 (m, 2H, H–C6, H–N3), 8.19 (s, 1H, H–C7), 10.39 (s, 1H, H–N2). ^{13}C NMR (126 MHz, DMSO- d_6 , δ (ppm)): 56.06 (OCH $_3$), 111.98 (C3), 121.02 (C1), 123.21 (C5), 126.26 (C6), 130.88 (C4), 136.08 (C7), 157.56 (C2), 157.62 (C8).

3-Methoxybenzaldehyde carbohydrazone (12)

White substance, recrystallized from methanol. Yield: 87%. m.p. 189 °C. Elemental analysis: Calculated for $\text{C}_9\text{H}_{12}\text{N}_4\text{O}_2$ (Mw = 208.38 g mol $^{-1}$): C, 58.81; H, 5.92; N, 27.43; O, 7.83%. Found: C, 58.15; H, 6.09; N, 27.27; O, 8.49%. IR (KBr, cm $^{-1}$) ν_{max} : 3326 m (NH $_2$), 3062 m (NH), 2997 m, 2837 m and 1454 m (O–CH $_3$), 1678 s (C=O), 1596 m (C=N), 1536 s and 1453 m (C=C arom.), 692 m and 783 m (C–H band (*meta*)). **Ratio E:Z isomers (75:25).** **Isomer E:** ^1H NMR (400 MHz, DMSO- d_6 , δ (ppm)): 3.80 (d, $J = 8.9$ Hz, 3H), 4.05 (s, 2H, H2–N4), 6.90 (d, 1H, H–C4, $^3J_{4,5} = 8.0$ Hz), 7.16–7.24 (m, 1H, H–C6), 7.28 (t, 1H, H–C5, $^3J_{5,4} = 8.0$ Hz), 7.41 (s, 1H, H–C2), 7.84 (s, 1H, H–N3), 8.16 (s, 1H, H–C7), 10.41 (s, 1H, H–N2). ^{13}C NMR (126 MHz, DMSO- d_6 , δ (ppm)): 55.70 (OCH $_3$), 110.93 (C2), 116.04 (C4), 120.33 (C6), 130.03 (C5), 136.66 (C1), 140.52 (C7), 157.56 (C3), 160.02 (C3). **Isomer Z:** ^1H NMR (400 MHz, DMSO- d_6 , δ (ppm)): 3.81 (d, $J = 8.9$ Hz, 3H), 4.05 (s, 2H, H2–N4), 6.97 (d, 1H, H–C4, $^3J_{4,5} = 7.9$ Hz), 7.35 (d, 2H, H–C5=H–C6, $^3J_{4,5} = 7.7$ Hz), 7.41 (s, 1H, H–C2), 7.84 (s, 1H, H–N3), 8.16 (s, 1H, H–C7), 10.76 (s, 1H, H–N2). ^{13}C NMR (126 MHz, DMSO- d_6 , δ (ppm)): 55.66 (OCH $_3$), 111.77 (C2), 115.90 (C4), 120.20 (C6), 130.23 (C5), 136.51 (C1), 143.55 (C7), 147.12 (C3), 152.51 (C3).

4-Methoxybenzaldehyde carbohydrazone (13)

White substance, recrystallized from methanol. Yield: 69%. m.p. 178 °C. Elemental analysis: Calculated for $C_9H_{12}N_4O_2$ (Mw = 208.38 $g\text{mol}^{-1}$): C, 58.81; H, 5.92; N, 27.43; O, 7.83%. Found: C, 58.33; H, 6.15; N, 27.88; O, 7.64%. IR (KBr, cm^{-1}) ν_{max} : 3300 m (NH_2), 3091 m (NH), 2952 m, 2834 m and 1421 m (O–CH₃), 1682 s (C=O), 1610 m (C=N), 1508 s and 1421 m (C–H arom.), 831 m (C–H bend (*para*)). **Isomer E**: ^1H NMR (400 MHz, DMSO- d_6 , δ (ppm)): 3.78 (s, 3H, O–CH₃), 4.07 (s, 2H, H₂–N₄), 6.94 (d, 2H, H–C₅=H–C₃, $^3J_{3,2} = ^3J_{5,6} = 7.8$ Hz), 7.68 (t, 2H, H–C₆=H–C₂, $^3J_{2,3} = ^3J_{6,5} = 7.8$ Hz), 7.80 (s, 1H, H–C₇), 7.95 (s, 1H, H–N₃), 10.25 (s, 1H, H–N₂). ^{13}C NMR (126 MHz, DMSO- d_6 , δ (ppm)): 55.72 (O–CH₃), 114.51 (C₃=C₅), 127.87 (C₁), 128.76 (C₂=C₆), 140.60 (C₇), 157.70 (C₈), 160.55 (C₄).

Lit. data: **E:Z isomers (85:15) Isomer E**: ^1H NMR (400 MHz, DMSO- d_6 , δ (ppm)): 3.76 (s, 3H, O–CH₃), 4.10 (s, 2H, H₂–N₄), 7.90 (s, 1H, H–C₇), 8.01 (d, 2H, H–C₅=H–C₃, $^3J_{3,2} = ^3J_{5,6} = 8.4$ Hz), 8.21 (d, 2H, H–C₆=H–C₂, $^3J_{2,3} = ^3J_{6,5} = 8.4$ Hz), 8.40 (s, 1H, H–N₃), 10.80 (s, 1H, H–N₂). **Isomer Z**: ^1H NMR (400 MHz, DMSO- d_6 , δ (ppm)): 3.76 (O–CH₃), 4.10 (s, 2H, H₂–N₄), 7.38 (s, 1H, H–C₇), 8.01 (d, 2H, H–C₅=H–C₃, $^3J_{3,2} = ^3J_{5,6} = 8.4$ Hz), 8.21 (d, 2H, H–C₆=H–C₂, $^3J_{2,3} = ^3J_{6,5} = 8.4$ Hz), 8.30 (s, 1H, H–N₃), 11.30 (s, 1H, H–N₂) (Okawara et al. 2006).

3-Chlorobenzaldehyde carbohydrazone (14)

White substance, recrystallized from methanol. Yield: 56%. m.p. 225 °C. Elemental analysis: Calculated for $C_8H_9N_4\text{OCl}$ (Mw = 212.70 $g\text{mol}^{-1}$): C, 45.19; H, 4.27; N, 26.35; O, 7.52; Cl, 16.67. Found: C, 45.02; H, 4.15; N, 26.88; O, 7.64; Cl, 16.31%. IR (KBr, cm^{-1}) ν_{max} : 3327 m (NH_2), 3089 m (NH), 1706 s (C=O), 1632 m (C=N), 1535 s and 1480 m (C=Carom.), 683 m and 790 m (C–H band (*meta*)), 757 m (C–Cl). ^1H NMR (400 MHz, DMSO- d_6 , δ (ppm)): 4.04 (s, 2H, H₂–N₄), 7.38 (d, 2H, H–C₃, H–C₅, $^3J_{5,6} = 6.6$ Hz) 7.60 (d, 2H, H–C₆, $^3J_{6,5} = 6.6$ Hz), 7.82 (s, 1H, H–C₂), 8.00 (s, 1H, H–C₇), 8.29 (s, 1H, H–N₃), 10.51 (s, 1H, H–N₂). ^{13}C NMR (126 MHz, DMSO- d_6 , δ (ppm)): 126.09 (C₂), 126.30 (C₄), 129.07 (C₅), 130.77 (C₆), 134.12 (C₃), 137.51 (C₁), 142.10 (C₇), 157.44 (C₈).

4-Chlorobenzaldehyde carbohydrazone (15)

White substance, recrystallized from ethanol. Yield: 53%. m.p. > 240 °C. Elemental analysis: Calculated for $C_8H_9N_4\text{OCl}$ (Mw = 212.70 $g\text{mol}^{-1}$): C, 45.19; H, 4.27; N, 26.35; O, 7.52; Cl, 16.67. Found: C, 45.64; H, 4.01; N, 26.55; O, 7.81; Cl, 15.99%. IR (KBr, cm^{-1}) ν_{max} : 3305 m (NH_2), 3091 m (NH), 1682 s (C=O), 1636 m

(C=N), 1518 s and 1491 m (C=Carom.), 829 m (C–H band (*para*)), 737 m (C–Cl). ^1H NMR (400 MHz, DMSO- d_6 , δ (ppm)): 4.07 (s, 2H, H₂–N₄), 7.43 (d, 2H, H–C₅=H–C₃, $^3J_{3,2} = ^3J_{5,6} = 8.05$ Hz), 7.79 (d, 2H, H–C₆=H–C₂, $^3J_{2,3} = ^3J_{6,5} = 8.05$ Hz), 7.84 (s, 1H, H–C₇), 8.12 (s, 1H, H–N₃), 10.46 (s, 1H, H–N₂). ^{13}C NMR (126 MHz, DMSO- d_6 , δ (ppm)): 128.80 (C₃=C₅), 129.02 (C₂=C₆), 133.86 (C₁), 134.23 (C₄), 139.17 (C₇), 157.47 (C₈) (Warkentin et al. 1977).

3-Bromobenzaldehyde carbohydrazone (16)

White substance, recrystallized from ethanol. Yield: 53%. m.p. 192–195 °C. Elemental analysis: Calculated for $C_8H_9N_4\text{OBr}$ (Mw = 257.15 $g\text{mol}^{-1}$): C, 37.38; H, 3.53; N, 21.79; O, 6.22; Br, 31.08. Found: C, 37.14; H, 3.71; N, 21.59; O, 6.77; Br, 30.79%. IR (KBr, cm^{-1}) ν_{max} : 3302 m (NH_2), 3088 m (NH), 1704 s (C=O), 1607 m (C=N), 1533 s and 1478 m (C=C arom.), 683 s and 788 m (C–H band (*meta*)), 577 m (C–Br). ^1H NMR (400 MHz, DMSO- d_6 , δ (ppm)): 4.10 (s, 2H, H₂–N₄), 7.32 (t, 1H, H–C₅, $^3J_{5,6} = 8.1$ Hz), 7.60 (d, 2H, H–C₄, $^3J_{4,5} = 8.1$ Hz), 7.60 (d, 2H, H–C₆, $^3J_{6,5} = 8.1$ Hz), 7.80 (s, 1H, H–C₂), 8.15 (s, 1H, H–C₇), 8.25 (s, 1H, H–N₃), 10.49 (s, 1H, H–N₂). ^{13}C NMR (126 MHz, DMSO- d_6 , δ (ppm)): 122.72 (C₂), 126.68 (C₃), 128.93 (C₄), 131.05 (C₅), 131.95 (C₆), 137.55 (C₁), 141.88 (C₇), 157.42 (C₈).

4-Bromobenzaldehyde carbohydrazone (17)

White substance, recrystallized from ethanol. Yield: 66%. m.p. 185 °C. Elemental analysis: Calculated for $C_8H_9N_4\text{OBr}$ (Mw = 257.15 $g\text{mol}^{-1}$): C, 37.38; H, 3.53; N, 21.79; O, 6.22; Br, 31.08. Found: C, 37.56; H, 3.66; N, 21.88; O, 6.46; Br, 30.44%. IR (KBr, cm^{-1}) ν_{max} : 3332 m (NH_2), 3098 m (NH), 1668 s (C=O), 1633 m (C=N), 1518 s and 1490 m (C=C arom.), 833 m (C–H band (*para*)), 593 m (C–Br). ^1H NMR (400 MHz, DMSO- d_6 , δ (ppm)): 4.03 (s, 2H, H₂–N₄), 7.56 (dd, 2H, H–C₅=H–C₃, $^3J_{3,2} = ^3J_{5,6} = 7.8$ Hz), 7.71 (dd, 2H, H–C₆=H–C₂, $^3J_{2,3} = ^3J_{6,5} = 7.8$ Hz), 7.82 (s, 1H, H–C₇), 8.14 (s, 1H, H–N₃), 10.47 (s, 1H, H–N₂). ^{13}C NMR (126 MHz, DMSO- d_6 , δ (ppm)): 122.58 (C₄), 129.06 (C₂=C₆), 131.93 (C₃=C₅), 134.57 (C₁), 139.32 (C₇), 157.45 (C₈).

4-Fluorobenzaldehyde carbohydrazone (18)

White substance, recrystallized from ethanol. Yield: 71%. m.p. 188 °C. Elemental analysis: Calculated for $C_8H_9FN_4\text{O}$ (Mw = 196.25 $g\text{mol}^{-1}$): C, 48.98; H, 4.62; N, 28.56; O, 8.16; F, 9.68%. Found: C, 48.81; H, 4.81; N, 28.77; O, 8.22; F, 9.39%. IR (KBr, cm^{-1}) ν_{max} : 3320 m (NH_2), 3084 m (NH), 1680 s (C=O), 1609 m (C=N), 1509 s and 1413 m (C=C

arom.), 1097 m (C–F), 839 m (C–H bend (*para*)). ^1H NMR (400 MHz, DMSO- d_6 , δ (ppm)): 4.08 (s, 2H, H2–N4), 7.10–7.26 (m, 2H, H–C5, H–C3), 7.71–7.92 (m, 3H, H–C7, H–C6, H–C2), 8.08 (s, 1H, H–N3), 10.39 (s, 1H, H–N2). ^{13}C NMR (126 MHz, DMSO- d_6 , δ (ppm)): 115.84 (C3), 116.06 (C3), 129.19 (C2), 129.27 (C6), 131.88 (C1), 139.36 (C7), 157.57 (C8), 164.47 (C4) (Warkentin et al. 1977).

Results and discussion

Synthesis and compound characterization

^1H and ^{13}C NMR spectra of newly synthesized derivatives of monocarbohydrazones showed good agreement with signals expected for hydrogen and carbon atoms. Also, spectra of compounds that are already known showed remarkably good superposition with the given literature data (Božić et al. 2017a, b; Okawara et al. 2006; Warkentin et al. 1977).

The results of the elemental analysis were within $\pm 0.5\%$ of the theoretical values. In the infrared spectra of monocarbohydrazones, absorptions between 1668 and 1718 cm^{-1} were assigned to the $\nu(\text{C}=\text{O})$ stretching. Signals recorded between 3062 and 3098 cm^{-1} were assigned to $\nu(\text{N}-\text{H})$ vibrations, while the absorptions between 1596 and 1645 cm^{-1} were attributed to the $\nu(\text{C}=\text{N})$ band. Giving the structure of all synthesized compounds, signals of $\nu(\text{C}=\text{C}$ arom.) are presented with two bands in the range of 1508–1593 and 1413–1491 cm^{-1} . The proof that all synthesized compounds belong to the group of monocarbohydrazones is expressed through the existence of $\nu(\text{NH}_2)$ vibrations that were recorded in the range of 3283–3361 cm^{-1} (Božić et al. 2017a, b).

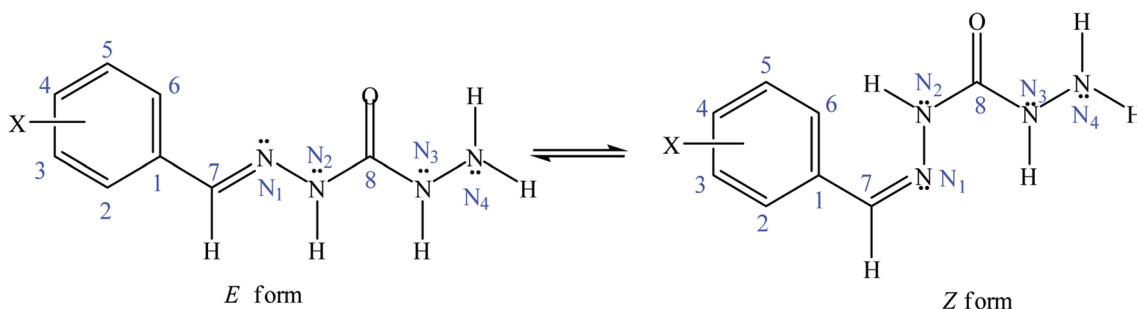
It is known that mCHs, as Schiff bases, show *E/Z* isomerization caused by the presence of the imino group (Okawara et al. 2006; Zelenin et al. 1999). Isomerization of synthesized monocarbohydrazones along the with numeration of atoms of interest is given in Scheme 2.

The assignment from NMR spectra indicated that the major product can also be an *E* and *Z* isomer. The ratio of

the integrals in ^1H NMR spectra pointed to the conclusion of the isomer ratio (*E/Z*). The stereochemistry of the mCHs, which have been found to possess both isomers, was undoubtedly established using 2D homonuclear (NOESY) and heteronuclear (HSQC and HMBC) NMR techniques. As an example, the chemical shifts of compound **10** were assigned by the combined use of one-dimensional (^1H and ^{13}C proton decoupled, Figs. S1 and S2 in ESM) and two-dimensional NMR experiments such as NOESY, HSQC, and HMBC given in Figs. S3–S5, respectively. In order to assess the conformation of compound **10** in a solution, the two-dimensional NOESY sequence was applied (Fig. S3). The *E* stereochemistry was assigned to be major isomer in DMSO d_6 solutions because the NOESY experiments show a correlation of C7–H and H–N2 and atoms (Fig. S3), which may be present only in the case of the *E* isomer (Scheme 2). Moreover, the chemical shifts of the proton present in *Z* isomer showed little difference to those found in the parent compound (Fig. S1). The 7.7:2.3 isomer ratio for compound **10** in DMSO d_6 was obtained from the ^1H NMR spectrum (Fig. S1). Analogously, the analyses of ^1H NMR data of N2–H proton were used for calculation of *E/Z* isomer ratio of other studied compounds. The obtained results showed that *E* form dominates in DMSO solution.

Geometry optimization of monocarbohydrazones

Carbohydrazones can exist in keto/enol tautomeric forms, and they could adopt *E* or *Z* configuration around the C=N bond (Božić et al. 2017b; Zelenin et al. 1999). Optimized geometries have shown that *E* isomers mainly adopt planar configurations with the angle between the phenyl group and carbohydrazide moiety around 14° (Table S1). Only in compound **8**, this angle is somewhat larger due to steric clash between bulky substituent in *ortho* position and hydrogen atom Hc (Schemes 1, 2 and Fig. S6). Much larger deviations from planarity exist in optimized geometries of *Z* isomers due to steric hindrance between ortho hydrogen (or substituent) on phenyl group and H1 hydrogen atom from carbohydrazide moiety; the angle between phenyl group and carbohydrazide moiety is in the range between 20.00 and 68.15°



Scheme 2 Isomerization of monocarbohydrazones with numeration of atoms of interest (Wiggins et al. 2009)

(Table S1). Energies obtained from ab initio calculations at MP2/6-311G(*d,p*) level of theory have shown that *Z* isomer is from 2.38 to 5.84 kcal/mol more stable for all compounds (Table S2), except for compound **2** where *E* configuration shows higher stability (0.15 kcal mol⁻¹) due to the formation of intermolecular hydrogen bond.

The effect of solvent on spectral behavior of monocarbohydrazones

The absorption spectra of the same molecule in the gaseous state and at the presence of a solvent always differ from one another. Depending on the properties of the solvent and its ability to enter into various physical or chemical interactions with the dissolved substance, a change in the absorption spectrum relative to the spectrum in the gaseous state is expected (Reichardt 2003). Intermolecular interactions and the effects of specific and nonspecific solvent–solute interactions on the UV absorption maxima shifts were studied by the method of linear solvation energy relationship (LSER).

There are a large number of models describing these interactions, but Kamlet–Taft's and Catalan's models are the most commonly used.

Kamlet–Taft's model is described by Eq. (1):

$$\nu = \nu_0 + s\pi^* + a\alpha + b\beta, \quad (1)$$

where ν is the frequency in a given solvent, ν_0 is the frequency in the standard solvent, π^* is dipolarity/polarizability, α acidity and β basicity of the solvent, while s , a and b are regression coefficients of the given equation (Taft and Kamlet 1976; Kamlet and Taft 1976; Kamlet et al. 1977).

Unlike Kamlet–Taft's, Catalan's model has separated the influence of the polarizability and dipolarity of the solvent,

so it contains another parameter more in the equation given below:

$$\nu = \nu_0 + aSA + bSB + cSP + dSdP, \quad (2)$$

where ν is the frequency in a given solvent, ν_0 is the solute property of the reference system, cyclohexane, SA represents the hydrogen bond donating ability (HBD), SB is a measure of the hydrogen bond accepting ability (HBA), SP describes the polarizability and SdP represents the dipolarity of the solvent. Correlation coefficients a , b , c and d describe the sensitivity of the absorption maxima to different types of solvent–solute interactions (Catalán and Hopf 2004; Catalán 2009).

Absorption spectra of carbohydrazones were recorded in the range from 200 to 400 nm in nineteen solvents of different properties. Figure 1 shows the absorption spectra of compound **4** in protic and aprotic solvents. For all other compounds, similar spectra were obtained.

Spectra of all investigated compounds show two or three absorption maxima. The first one occurs at about 220 nm, but it was excluded from further analysis because some solvents in that part of the spectrum absorb electromagnetic radiation and overlap the spectrum of the compound. The second one, used for analysis, occurs in the range from 280 to 330 nm, depending on the substituent present and solvent used. After the process of deconvolution of the absorption spectra, only one absorption maximum was observed in all solvents. It is assumed that the analyzed maxima come as a result of $n \rightarrow \pi^*$ transition in molecules. Due to the diversity of substituents present, the absorption maxima of compounds tested occur in a wide range of wavelengths. Absorption frequencies at the maximum of absorbance and the values of observed molar absorptivity for all compounds

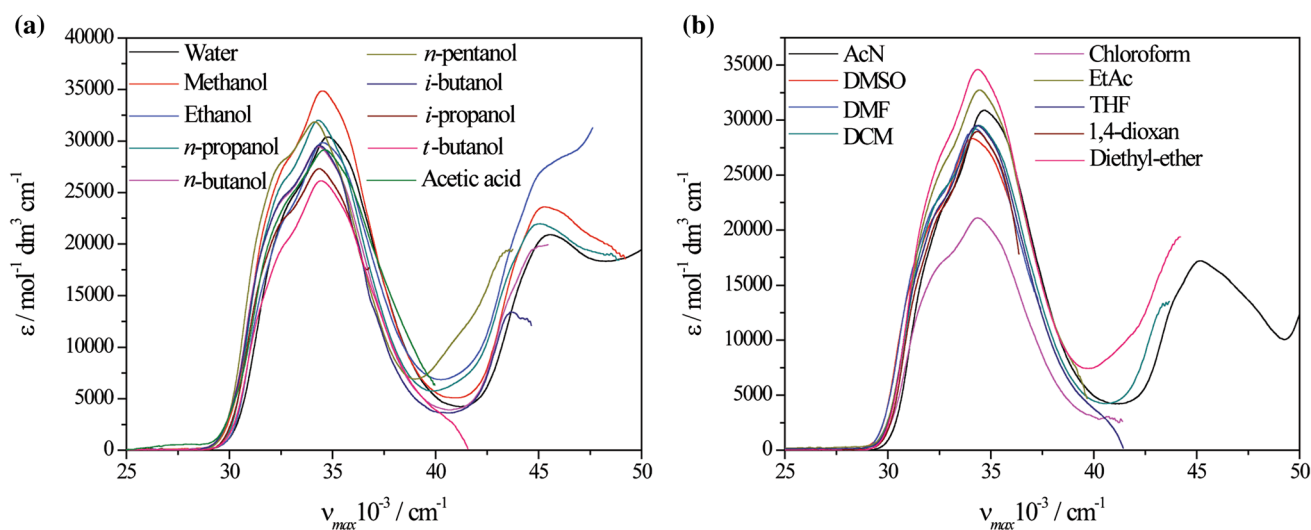


Fig. 1 Spectra of compound **4** in protic (a) and aprotic (b) solvents

Table 1 Absorption frequencies, $\nu_{\max} \times 10^{-3}$ (cm^{-1}) and values of molar absorptivity, ϵ ($\text{mol}^{-1} \text{dm}^3 \text{cm}^{-1}$), in protic solvents

Com-pound/solvent	Water	Methanol	Ethanol	<i>n</i> -Propanol	<i>n</i> -Butanol	<i>n</i> -Pentanol	<i>i</i> -Butanol	<i>i</i> -Propanol	<i>t</i> -Butanol	Acetic acid
1	35.41 (20,545)	35.26 (24,659)	35.17 (21,153)	35.12 (22,252)	35.10 (20,802)	35.06 (21,936)	35.06 (21,186)	35.12 (22,636)	34.99 (22,146)	35.21 (23,282)
2	36.06 (20,374)	35.92 (19,278)	35.90 (18,033)	35.85 (19,966)	35.84 (13,834)	35.82 (14,003)	35.84 (46,060)	35.83 (17,222)	35.780 (1,425)	35.88 (20,713)
3	35.38 (16,149)	35.16 (16,678)	35.14 (16,323)	35.11 (16,180)	35.08 (15,169)	34.97 (17,405)	35.00 (15,722)	35.00 (16,037)	34.83 (11,953)	35.14 (16,709)
4	34.50 (30,425)	34.35 (34,794)	34.30 (29,895)	34.31 (31,942)	34.31 (29,463)	34.21 (31,835)	34.25 (29,536)	34.26 (27,302)	34.19 (26,145)	34.27 (29,175)
5	35.275 (2,201)	34.86 (25,747)	34.84 (23,567)	34.74 (25,060)	34.67 (23,342)	34.62 (24,527)	34.71 (24,078)	34.64 (22,388)	34.47 (20,868)	34.80 (23,402)
6	35.13 (23,840)	34.93 (25,418)	34.86 (24,589)	34.80 (25,163)	34.73 (24,399)	34.72 (24,107)	34.80 (24,845)	34.74 (23,110)	34.65 (22,799)	34.88 (24,364)
7	34.93 (17,531)	34.68 (25,160)	34.59 (24,151)	34.59 (25,103)	34.57 (27,664)	34.52 (25,636)	34.58 (27,914)	34.56 (25,524)	34.47 (23,247)	34.65 (25,588)
8	37.15 (17,463)	36.92 (13,064)	36.84 (14,588)	36.82 (15,195)	36.83 (13,789)	36.86 (11,443)	36.79 (13,444)	36.78 (11,747)	36.75 (11,042)	36.90 (18,098)
9	34.21 (13,980)	33.76 (24,261)	33.64 (25,679)	33.52 (23,007)	33.46 (25,636)	33.30 (24,948)	33.26 (23,299)	33.30 (21,065)	33.00 (22,623)	33.65 (26,237)
10	30.92 (16,070)	30.74 (11,672)	30.67 (11,552)	30.54 (12,659)	30.49 (14,553)	30.43 (11,076)	30.38 (14,201)	30.37 (10,367)	30.33 (11,042)	30.69 (21,194)
11	35.92 (15,398)	35.85 (17,023)	35.75 (18,131)	35.72 (14,596)	35.69 (16,844)	35.66 (14,759)	35.73 (12,493)	35.70 (14,347)	35.61 (13,568)	35.78 (15,802)
12	35.34 (20,015)	35.13 (22,181)	35.12 (21,460)	35.06 (20,440)	35.07 (21,796)	35.00 (21,757)	35.05 (18,907)	35.07 (20,309)	34.93 (21,031)	35.14 (21,629)
13	34.67 (22,567)	34.52 (25,418)	34.45 (24,144)	34.45 (24,676)	34.48 (24,871)	34.44 (23,296)	34.46 (21,251)	34.45 (21,833)	34.35 (24,536)	34.50 (24,078)
14	33.40 (8,526)	33.03 (23,972)	32.90 (23,623)	33.02 (21,357)	32.84 (22,587)	32.81 (21,406)	32.94 (17,597)	32.89 (20,425)	32.76 (22,473)	32.96 (20,149)
15	34.86 (19,658)	34.72 (24,003)	34.65 (22,657)	34.58 (23,180)	34.58 (22,150)	34.59 (21,843)	34.61 (19,771)	34.58 (19,416)	34.53 (19,665)	34.66 (23,751)
16	33.33 (34,075)	33.13 (22,984)	33.05 (20,335)	33.03 (19,141)	32.99 (20,132)	32.95 (19,781)	33.03 (14,812)	33.00 (17,726)	32.84 (19,916)	33.08 (19,399)
17	34.79 (23,479)	34.65 (25,418)	34.52 (35,206)	34.52 (24,665)	34.43 (24,244)	34.40 (22,371)	34.52 (39,639)	34.47 (26,009)	34.34 (24,072)	34.57 (25,404)
18	35.63 (17,612)	35.41 (15,659)	35.34 (22,345)	35.27 (17,165)	35.27 (21,714)	35.24 (23,203)	35.30 (19,416)	35.27 (17,167)	35.20 (15,412)	35.35 (21,317)

Table 2 Absorption frequencies, $\nu_{\max} \times 10^{-3}$ (cm⁻¹) and values of molar absorptivity, ϵ (mol⁻¹ dm³ cm⁻¹), in aprotic solvents

Com- pound/ solvent	AcN	DMSO	DMF	DCM	Chloroform	EtAc	THF	1,4-Dioxane	Diethyl ether
1	35.06 (21,450)	35.01 (20,753)	34.98 (20,335)	34.93 (21,793)	34.91 (20,412)	34.92 (21,054)	34.87 (20,215)	34.82 (20,825)	34.80 (25,155)
2	35.80 (20,137)	35.78 (18,557)	35.74 (18,098)	35.77 (20,640)	35.66 (14,960)	35.69 (22,396)	35.66 (17,522)	35.58 (14,278)	35.55 (23,754)
3	34.94 (15,864)	34.86 (14,914)	34.82 (14,788)	34.79 (15,968)	34.78 (11,042)	34.74 (17,088)	34.72 (13,992)	34.67 (15,085)	34.65 (19,099)
4	34.23 (30,865)	34.20 (28,282)	34.19 (29,227)	34.16 (29,548)	34.13 (21,186)	34.07 (32,732)	34.08 (29,487)	34.05 (28,965)	34.01 (34,662)
5	34.59 (23,239)	34.54 (18,350)	34.50 (22,483)	34.46 (24,210)	34.42 (23,015)	34.44 (25,357)	34.33 (22,494)	34.28 (23,393)	34.20 (27,288)
6	34.71 (24,244)	34.66 (24,227)	34.64 (23,806)	34.59 (25,679)	34.59 (22,397)	34.55 (26,340)	34.52 (24,244)	34.49 (23,668)	34.48 (29,519)
7	34.51 (27,264)	34.46 (23,230)	34.43 (27,706)	34.39 (27,706)	34.32 (23,608)	34.29 (28,591)	34.27 (26,305)	34.26 (26,881)	34.20 (28,893)
8	36.80 (16,456)	36.72 (15,829)	36.71 (13,381)	36.68 (15,767)	36.65 (15,195)	36.62 (17,826)	36.58 (13,176)	36.54 (12,135)	36.51 (15,836)
9	33.37 (25,060)	33.08 (24,433)	32.94 (24,407)	32.91 (27,199)	32.69 (25,172)	32.63 (27,930)	32.61 (24,877)	32.31 (20,883)	32.22 (25,369)
10	30.39 (12,125)	30.32 (9,243)	30.27 (13,368)	30.23 (14,588)	30.24 (10,004)	30.17 (22,088)	30.12 (12,232)	30.14 (12,211)	30.07 (13,958)
11	35.66 (16,012)	35.60 (11,987)	35.58 (14,519)	35.52 (14,622)	35.54 (14,112)	35.51 (18,021)	35.48 (14,215)	35.46 (16,879)	35.394 (1,924)
12	34.97 (21,607)	34.95 (18,610)	34.91 (14,476)	34.88 (19,615)	34.88 (19,831)	34.84 (28,290)	34.81 (18,310)	34.78 (19,250)	34.72 (22,234)
13	34.39 (24,768)	34.37 (20,876)	34.34 (23,210)	34.32 (23,031)	34.28 (22,494)	34.23 (23,900)	34.23 (22,165)	34.19 (23,323)	34.18 (26,638)
14	32.84 (23,104)	32.81 (19,099)	32.73 (21,564)	32.67 (20,992)	32.71 (20,193)	32.62 (24,659)	32.67 (21,062)	32.56 (20,412)	32.48 (24,296)
15	34.55 (22,424)	34.51 (18,608)	34.47 (17,898)	34.41 (22,945)	34.40 (20,335)	34.41 (23,147)	34.31 (19,426)	34.33 (21,184)	34.27 (22,473)
16	32.96 (20,600)	32.92 (16,542)	32.85 (17,640)	32.86 (20,367)	32.75 (18,532)	32.79 (23,228)	32.77 (19,393)	32.68 (18,522)	32.60 (18,625)
17	34.42 (23,926)	34.38 (22,015)	34.32 (21,778)	34.32 (24,273)	34.27 (23,147)	34.25 (26,983)	34.22 (23,917)	34.22 (23,303)	34.17 (27,292)
18	35.22 (17,715)	35.18 (19,510)	35.14 (36,312)	35.13 (20,753)	35.07 (19,031)	35.04 (16,598)	35.05 (19,582)	35.02 (14,565)	34.98 (23,299)

in protic and aprotic compounds are shown in Tables 1 and 2, respectively.

Based on the results shown in Tables 1 and 2, it is clear that the hypsochromic displacement of the absorption maxima occurs with increasing the polarity of the solvent. This is characteristic of $n \rightarrow \pi^*$ transitions in molecules (Antić-Jovanović 2006). Table 3 shows the empirical parameters of the solvents used: E_T^N —empirical polarity parameter, Kamlet–Taft's and Catalan's solvent parameters and Hansen's solubility parameters: δd —energy from dispersion forces, δp —energy from dipolar intermolecular forces, δh —energy from hydrogen bonds between molecules.

In Fig. 2, the correlation of the absorption maxima of compound 4 with empirical polarity parameter, E_T^N , is

shown. As can be seen, the hypsochromic shifting of absorption maxima is represented. This dependency also confirms the previously stated assumption that the observed absorption maxima of the investigated compounds originate from the $n \rightarrow \pi^*$ transition in the molecule (Antić-Jovanović 2006).

A quantitative description of the interactions between the investigated compounds and the surrounding medium is obtained with two models. Correlations of absorption maxima with Kamlet–Taft's parameters (Table 3) are given in Eq. (1), and the values of their regression coefficients, as well as the statistical parameters, are given in Table 4.

By observing the values of the correlation coefficients of equations for each compound ($r^2=0.915\text{--}0.971$), it

Table 3 Parameters of the solvents used (Antić–Jovanović 2006; Catalán and Hopf 2004; Catalán 2009; Hansen 2007; Kamlet and Taft 1976; Kamlet et al. 1977; Taft and Kamlet 1976)

Solvent	E_T^N	Kamlet–Taft's solvent parameters			Catalan's solvent parameters				Hansen's solubility parameters		
		α	β	π	SA	SB	SP	SdP	δ_d	δ_p	δ_h
Water	1.000	1.17	0.47	1.09	1.062	0.025	0.681	0.997	15.6	16.0	42.3
Methanol	0.762	0.98	0.66	0.60	0.605	0.545	0.608	0.904	15.1	12.3	22.3
Ethanol	0.654	0.86	0.75	0.54	0.400	0.658	0.633	0.783	15.8	8.8	19.4
<i>n</i> -Propanol	0.617	0.84	0.90	0.52	0.367	0.782	0.658	0.748	16.0	6.8	17.4
<i>n</i> -Butanol	0.586	0.84	0.84	0.47	0.341	0.809	0.674	0.655	16.0	5.7	15.8
<i>n</i> -Pentanol	0.568	0.84	0.86	0.40	0.319	0.860	0.687	0.587	–	–	–
<i>i</i> -Butanol	0.552	0.79	0.84	0.40	0.311	0.828	0.657	0.684	15.1	5.7	15.9
<i>i</i> -Propanol	0.546	0.76	0.84	0.48	0.283	0.830	0.633	0.808	15.8	6.1	16.4
<i>t</i> -Butanol	0.389	0.42	0.93	0.41	0.145	0.928	0.632	0.732	–	–	–
Acetic acid	0.648	1.12	0.45	0.64	0.689	0.390	0.651	0.676	14.5	8.0	13.5
AcN	0.460	0.19	0.40	0.75	0.044	0.286	0.645	0.974	15.3	18.0	6.1
DMSO	0.444	0.00	0.76	1.00	0.072	0.647	0.830	1.000	18.4	16.4	10.2
DMF	0.386	0.00	0.69	0.88	0.031	0.613	0.759	0.977	17.4	13.7	11.3
DCM	0.319	0.13	0.10	0.82	0.040	0.178	0.761	0.769	18.2	6.3	6.1
Chloroform	0.259	0.44	0.00	0.58	0.047	0.071	0.783	0.614	17.8	3.1	5.7
EtAc	0.228	0.00	0.45	0.55	0.000	0.542	0.656	0.603	15.8	5.3	7.2
THF	0.207	0.00	0.55	0.58	0.000	0.591	0.714	0.634	16.8	5.7	8.0
1,4-Dioxane	0.164	0.00	0.37	0.55	0.000	0.444	0.737	0.312	19.0	1.8	7.4
Diethyl ether	0.117	0.00	0.47	0.27	0.000	0.562	0.617	0.385	14.5	2.9	5.1

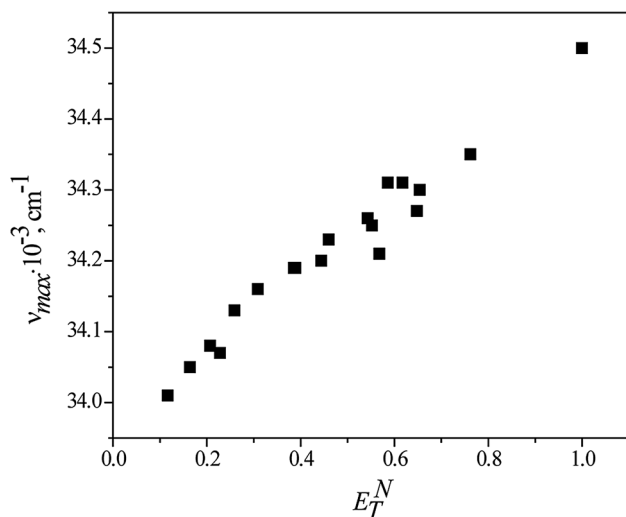


Fig. 2 Correlation obtained between absorption frequencies of compound 4 with empirical parameter of the solvents used

can be concluded that the model used is suitable for the interpretation of solvent–solute interactions of synthesized carbohydrazones.

The highest values are obtained for regression coefficient *s*, which indicates that the polarizability/dipolarity of the solvents has the greatest impact on the spectral shifting of investigated compounds. (Exceptions are compounds **3**, **10** and **11** where coefficient *a* has the biggest value.) A

slightly lower influence has the acidity of the solvent (values of the regression coefficient *a*), while the smallest impact on the maxima shifting of all carbohydrazones has alkalinity, described with regression coefficient *b*. A positive sign in front of each of these regression coefficients indicates that with the increase in polarizability/dipolarity, acidity and alkalinity of the solvent, hypsochromic shifting of the absorption maxima of the tested compounds is expected.

In addition to the Kamlet–Taft's, for the description of the solvent–solute interactions of the investigated carbohydrazones, Catalan's model was also used. Results for the tested compounds, in all solvents, obtained by applying this model are shown in Table 5.

By observing the results of Catalan's model, it can be noticed that the regression coefficient *a* has the highest value (with exception for compounds **9** and **11**, where solvent's polarizability has the most dominant effect), which means that the acidity of the solvent has the greatest influence on the spectral behavior of the carbohydrazones. Slightly smaller effects have polarizability and dipolarity of solvent (coefficient values *c* and *d*). In the end, as with Kamlet–Taft's model, the smallest influence has the alkalinity of the solvent—coefficient *b* has the least value for all compounds. The positive sign in front of the regression coefficients *a*, *b* and *d* means that hypsochromic shifting of the absorption maxima will occur in case of an increase in the acidity, basicity, and dipolarity of the solvent. The negative sign in front of the coefficient *c* indicates that with

Table 4 Regression coefficients of the obtained equations by Kamlet–Taft's model

Compound	$\nu_0 \times 10^{-3}, \text{cm}^{-1}$	$a \times 10^{-3}, \text{cm}^{-1}$	$b \times 10^{-3}, \text{cm}^{-1}$	$s \times 10^{-3}, \text{cm}^{-1}$	r^2 ^a	SD ^b	F^c
1	34.634 (±0.043)	0.298 (±0.024)	0.097 (±0.041)	0.335 (±0.048)	0.940	0.042	78
2	35.436 (±0.039)	0.218 (±0.021)	0.111 (±0.037)	0.290 (±0.043)	0.923	0.037	60
3	34.458 (±0.049)	0.398 (±0.027)	0.115 (±0.047)	0.350 (±0.055)	0.952	0.048	99
4	33.876 (±0.034)	0.214 (±0.019)	0.103 (±0.032)	0.282 (±0.038)	0.935	0.033	72
5	33.950 (±0.072)	0.472 (±0.040)	0.116 (±0.068)	0.571 (±0.080)	0.934	0.069	71
6	34.295 (±0.048)	0.327 (±0.027)	0.076 (±0.046)	0.341 (±0.054)	0.934	0.047	71
7	33.993 (±0.043)	0.332 (±0.024)	0.145 (±0.041)	0.402 (±0.048)	0.955	0.041	105
8	36.360 (±0.044)	0.288 (±0.024)	0.090 (±0.042)	0.339 (±0.049)	0.934	0.043	71
9	31.747 (±0.156)	0.962 (±0.086)	0.409 (±0.147)	1.129 (±0.173)	0.929	0.150	66
10	29.860 (±0.074)	0.466 (±0.041)	0.071 (±0.069)	0.433 (±0.082)	0.921	0.071	58
11	35.292 (±0.040)	0.269 (±0.022)	0.100 (±0.038)	0.255 (±0.044)	0.935	0.038	72
12	34.590 (±0.029)	0.299 (±0.016)	0.094 (±0.028)	0.310 (±0.033)	0.971	0.028	165
13	34.041 (±0.028)	0.243 (±0.016)	0.107 (±0.027)	0.263 (±0.031)	0.962	0.027	126
14	32.255 (±0.068)	0.374 (±0.038)	0.131 (±0.064)	0.503 (±0.076)	0.915	0.066	54
15	34.129 (±0.045)	0.279 (±0.025)	0.129 (±0.043)	0.303 (±0.051)	0.928	0.044	65
16	32.440 (±0.049)	0.315 (±0.027)	0.134 (±0.047)	0.415 (±0.055)	0.936	0.048	73
17	34.004 (±0.051)	0.312 (±0.028)	0.085 (±0.048)	0.331 (±0.057)	0.922	0.049	60
18	34.798 (±0.045)	0.301 (±0.025)	0.105 (±0.043)	0.342 (±0.050)	0.936	0.043	74

^aCorrelation coefficient^bStandard deviation^cFisher's correlation test**Table 5** Regression coefficients of Catalan's model

Compound	$\nu_0 \times 10^{-3}, \text{cm}^{-1}$	$a \times 10^{-3}, \text{cm}^{-1}$	$b \times 10^{-3}, \text{cm}^{-1}$	$c \times 10^{-3}, \text{cm}^{-1}$	$d \times 10^{-3}, \text{cm}^{-1}$	r^2	SD	F	Solvents excluded
1	34.866 (±0.104)	0.416 (±0.030)	0.035 (±0.029)	−0.232 (±0.140)	0.290 (±0.041)	0.971	0.030	119	–
2	35.671 (±0.136)	0.281 (±0.036)	0.045 (±0.033)	−0.214 (±0.170)	0.239 (±0.046)	0.938	0.032	46	b, c
3	34.916 (±0.253)	0.528 (±0.067)	– ^a	−0.423 (±0.316)	0.219 (±0.086)	0.926	0.059	38	b, c
4	33.905 (±0.133)	0.310 (±0.039)	0.055 (±0.037)	–	0.247 (±0.052)	0.919	0.038	40	–
5	34.164 (±0.227)	0.701 (±0.066)	–	–	0.391 (±0.089)	0.946	0.065	61	–
6	34.522 (±0.118)	0.470 (±0.036)	–	−0.190 (±0.159)	0.259 (±0.046)	0.967	0.034	104	–
7	34.324 (±0.160)	0.456 (±0.042)	0.052 (±0.039)	−0.252 (±0.200)	0.277 (±0.054)	0.961	0.041	73	b, c
8	36.459 (±0.155)	0.419 (±0.046)	–	–	0.262 (±0.061)	0.933	0.044	48	–
9	33.149 (±0.617)	1.123 (±0.163)	–	−1.460 (±0.772)	0.953 (±0.210)	0.929	0.144	39	b, c
10	30.452 (±0.288)	0.620 (±0.076)	–	−0.525 (±0.360)	0.230 (±0.098)	0.931	0.067	40	b, c
11	35.708 (±0.136)	0.324 (±0.036)	0.036 (±0.032)	−0.439 (±0.170)	0.192 (±0.046)	0.952	0.032	60	b, c
12	34.651 (±0.146)	0.439 (±0.043)	0.068 (±0.041)	–	0.231 (±0.057)	0.940	0.042	55	–
13	34.038 (±0.130)	0.361 (±0.038)	0.087 (±0.037)	–	0.219 (±0.051)	0.933	0.037	49	–
14	32.321 (±0.217)	0.574 (±0.064)	–	–	0.360 (±0.085)	0.928	0.062	45	–
15	34.444 (±0.173)	0.372 (±0.046)	0.062 (±0.042)	−0.303 (±0.216)	0.233 (±0.059)	0.937	0.040	44	b, c
16	32.775 (±0.176)	0.421 (±0.047)	–	0.268 (±0.220)	0.297 (±0.060)	0.948	0.041	55	b, c
17	34.393 (±0.171)	0.411 (±0.045)	–	−0.367 (±0.213)	0.229 (±0.058)	0.948	0.040	55	b, c
18	35.140 (±0.126)	0.414 (±0.033)	–	−0.287 (±0.157)	0.226 (±0.043)	0.970	0.029	97	b, c

^aError greater than the value^bEthyl acetate^cDiethyl ether

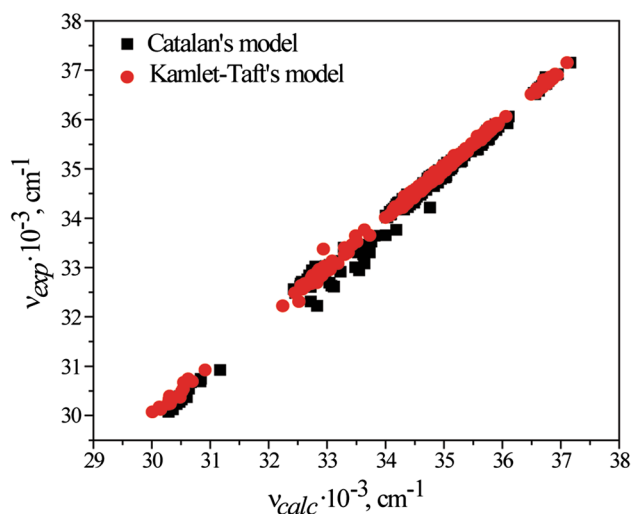


Fig. 3 Correlation of ν_{exp} with ν_{calc}

the increase in polarizability of the solvent bathochromic shifting of the maxima will occur.

The correctness of the applied models was confirmed by obtaining linear dependences with good correlation coefficients between experimentally determined (ν_{exp}) and

theoretically calculated absorption frequencies (ν_{calc}) based on Eqs. (1) and (2). Dependencies obtained are shown in Fig. 3.

Correlation coefficient for Kamlet–Taft's model was $r^2 = 0.998$ and for Catalan's was $r^2 = 0.993$ (Fig. 3). Judging by the values, both models applied are suitable for the interpretation of the effect of the solvent on maxima shifting of the tested monocarbohydrazones (Bauer et al. 2008; Riedel and Spange 2012). By observing the numerical values of the regression coefficients within Kamlet–Taft's model, it can be concluded that the influences of polarizability/dipolarity and acidity of the solvents are almost equal, while Catalan's model shows that acidity has a principal impact on maxima shifting of the monocarbohydrazones. (Exceptions are compounds **9** and **11**, where solvents' polarizability has the most dominant effect.) On the first site, two models show different results that can be explained with the fact that the influence of the polarizability/dipolarity (π^*) within Kamlet–Taft's model is divided into two scales when Catalan's model is observed—SP and SdP scales. The sum of shares of all nonspecific interactions (dipolarity and polarizability) obtained by Catalan's model prevails over the acidity of the solvents used and that is in agreement with the results of Kamlet–Taft's model.

Table 6 Results of correlations with Hansen's solubility parameters

Comp.	$\nu_0 \times 10^{-3}, \text{cm}^{-1}$	$d \times 10^{-3}, \text{cm}^{-1}$	$p \times 10^{-3}, \text{cm}^{-1}$	$h \times 10^{-3}, \text{cm}^{-1}$	r^2	SD	F	Solvents excluded
1	35.568 (± 0.179)	-0.043 (± 0.010)	0.006 (± 0.002)	0.011 (± 0.002)	0.926	0.047	46	a, b
2	36.227 (± 0.144)	-0.036 (± 0.008)	0.006 (± 0.002)	0.008 (± 0.001)	0.928	0.037	48	a, b, c
3	35.818 (± 0.276)	-0.064 (± 0.015)	–	0.013 (± 0.002)	0.903	0.070	34	a, d
4	34.527 (± 0.126)	-0.026 (± 0.007)	0.003 (± 0.002)	0.008 (± 0.001)	0.934	0.032	47	a, b, d
5	35.117 (± 0.269)	-0.050 (± 0.015)	0.007 (± 0.004)	0.020 (± 0.002)	0.933	0.071	56	A
6	35.299 (± 0.200)	-0.047 (± 0.011)	0.005 (± 0.003)	0.012 (± 0.002)	0.930	0.050	49	a, d
7	35.046 (± 0.214)	-0.046 (± 0.012)	0.006 (± 0.003)	0.012 (± 0.002)	0.925	0.054	45	a, d
8	37.239 (± 0.155)	-0.039 (± 0.009)	0.006 (± 0.002)	0.010 (± 0.001)	0.944	0.039	56	a, b, d
9	35.626 (± 0.631)	-0.175 (± 0.035)	0.020 (± 0.009)	0.025 (± 0.005)	0.917	0.158	37	a, b, d
10	30.833 (± 0.371)	-0.042 (± 0.020)	0.006 (± 0.005)	0.016 (± 0.003)	0.907	0.080	26	a, b, d, e, f
11	36.328 (± 0.168)	-0.049 (± 0.009)	0.003 (± 0.002)	0.008 (± 0.001)	0.922	0.042	43	a, d
12	35.543 (± 0.199)	-0.042 (± 0.011)	–	0.010 (± 0.002)	0.910	0.050	37	a, d
13	34.912 (± 0.137)	-0.038 (± 0.008)	0.003 (± 0.002)	0.007 (± 0.001)	0.934	0.034	47	a, b, d
14	33.272 (± 0.240)	-0.042 (± 0.013)	0.006 (± 0.003)	0.016 (± 0.002)	0.929	0.060	48	a, d
15	35.025 (± 0.138)	-0.040 (± 0.008)	0.005 (± 0.002)	0.009 (± 0.001)	0.946	0.036	64	a, b
16	33.560 (± 0.196)	-0.049 (± 0.011)	0.006 (± 0.003)	0.011 (± 0.002)	0.930	0.049	49	a, d
17	35.021 (± 0.218)	-0.047 (± 0.012)	0.004 (± 0.002)	0.012 (± 0.001)	0.909	0.055	36	a, d
18	35.676 (± 0.163)	-0.039 (± 0.009)	0.004 (± 0.002)	0.012 (± 0.001)	0.947	0.041	65	a, d

^aDiethyl ether

^bTHF

^cDCM

^dEtAc

^eCH₃COOH

^fEtOH

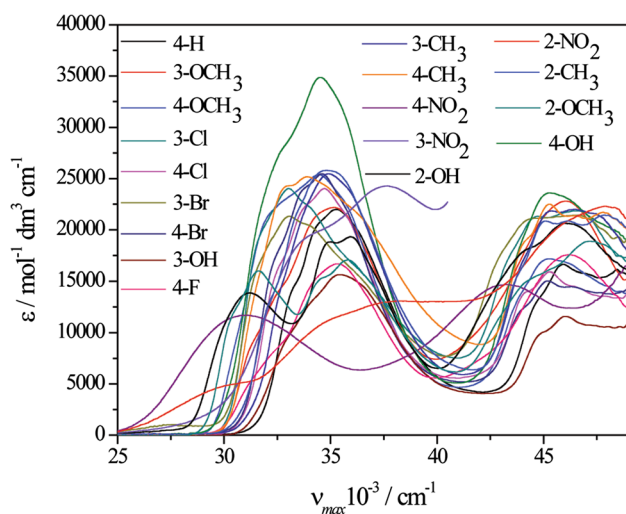


Fig. 4 Spectra of all investigated compounds recorded in methanol

Table 7 Hammett's constants of substituents

Substituent	$\sigma_{m,p}$	Substituent	$\sigma_{m,p}$	Substituent	$\sigma_{m,p}$
4-H	0.00	3-Br	0.39	3-CH ₃	-0.07
4-F	0.06	3-NO ₂	0.71	4-CH ₃	-0.17
4-Cl	0.23	4-NO ₂	0.78	4-OCH ₃	-0.27
4-Br	0.23	3-OCH ₃	0.12	4-OH	-0.37
3-Cl	0.37	3-OH	0.12		

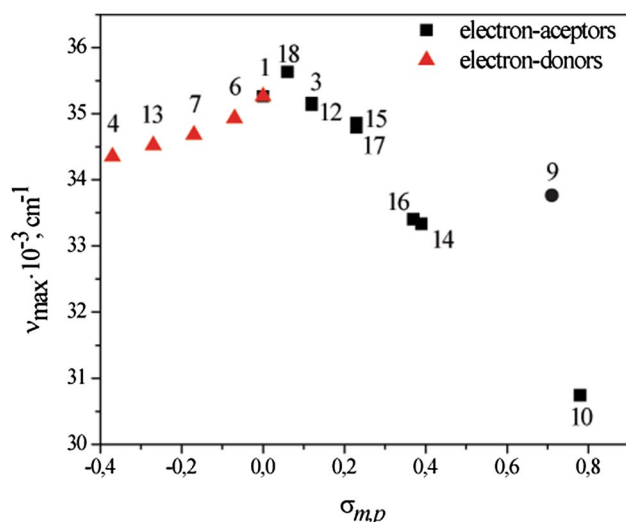


Fig. 5 Dependences of absorption frequencies from constants of substituents in methanol

In addition to the effect of solvent, correlations of the absorption maxima (Tables 1, 2) with Hansen's solubility parameters (Table 3) were made in order to obtain additional information about the interactions that occur between

Table 8 Regression coefficients of Hammett's equation for all solvents used

Solvent	$\nu_0 \times 10^{-3}, \text{cm}^{-1}$	$\rho \times 10^{-3}, \text{cm}^{-1}$	r^2	SD
Electron acceptors				
Water	35.974(±0.154)	-6.395(±0.454)	-0.983	0.304
Methanol	35.781(±0.167)	-6.433(±0.494)	-0.980	0.330
Ethanol	35.716(±0.175)	-6.470(±0.515)	-0.979	0.345
<i>n</i> -Propanol	35.691(±0.164)	-6.507(±0.484)	-0.981	0.324
<i>n</i> -Butanol	35.670(±0.174)	-6.601(±0.513)	-0.979	0.343
<i>n</i> -Pentanol	35.625(±0.175)	-6.599(±0.517)	-0.979	0.346
<i>i</i> -Butanol	35.690(±0.179)	-6.659(±0.526)	-0.979	0.352
<i>i</i> -Propanol	35.691(±0.169)	-6.715(±0.498)	-0.981	0.333
<i>t</i> -Butanol	35.556(±0.175)	-6.634(±0.517)	-0.979	0.346
Acetic acid	35.739(±0.169)	-6.459(±0.498)	-0.980	0.333
AcN	35.616(±0.169)	-6.607(±0.498)	-0.981	0.333
DMSO	35.576(±0.170)	-6.628(±0.981)	-0.981	0.335
DMF	35.535(±0.171)	-6.664(±0.503)	-0.981	0.336
DCM	35.506(±0.174)	-6.668(±0.513)	-0.980	0.343
Chloroform	35.475(±0.171)	-6.635(±0.504)	-0.980	0.337
EtAc	35.465(±0.174)	-6.696(±0.512)	-0.980	0.342
THF	35.439(±0.164)	-6.701(±0.483)	-0.982	0.323
1,4-Dioxane	35.395(±0.179)	-6.668(±0.527)	-0.979	0.353
Diethyl ether	35.359(±0.178)	-6.735(±0.524)	-0.979	0.351
Electron donors				
Water	35.352 (±0.040)	2.407 (±0.183)	0.991	0.055
Methanol	35.160 (±0.175)	2.340 (±0.302)	0.976	0.090
Ethanol	35.071 (±0.069)	2.256 (±0.314)	0.972	0.094
<i>n</i> -Propanol	35.017 (±0.068)	2.063 (±0.306)	0.968	0.091
<i>n</i> -Butanol	34.974 (±0.082)	1.906 (±0.371)	0.948	0.110
<i>n</i> -Pentanol	34.955 (±0.072)	2.073 (±0.327)	0.965	0.097
<i>i</i> -Butanol	34.993 (±0.046)	2.064 (±0.210)	0.985	0.063
<i>i</i> -Propanol	34.995 (±0.081)	2.099 (±0.366)	0.957	0.109
<i>t</i> -Butanol	34.879 (±0.071)	1.986 (±0.322)	0.963	0.096
Acetic acid	35.120 (±0.059)	2.376 (±0.269)	0.981	0.080
AcN	34.944 (±0.075)	2.069 (±0.340)	0.962	0.101
DMSO	34.891 (±0.078)	1.994 (±0.355)	0.956	0.106
DMF	34.861 (±0.079)	1.962 (±0.356)	0.954	0.106
DCM	34.810 (±0.080)	1.887 (±0.361)	0.949	0.108
Chloroform	34.789 (±0.087)	1.951 (±0.396)	0.943	0.118
EtAc	34.782 (±0.095)	2.105 (±0.429)	0.943	0.128
THF	34.737 (±0.093)	1.947 (±0.420)	0.937	0.125
1,4-Dioxane	34.700 (±0.082)	1.919 (±0.371)	0.948	0.111
Diethyl ether	34.679 (±0.090)	1.961 (±0.406)	0.941	0.121

the investigated compounds and the surrounding medium. Correlations were made by the method of multiple linear correlations according to Eq. (3):

$$\nu = \nu_0 + d\delta d + p\delta p + h\delta h, \quad (3)$$

Table 9 Calculated values of Λ index, Q_{CT} and D_{CT} during electron excitation

Compound	Λ index	Q_{CT} (e ⁻)	D_{CT} (Å)
1	0.73	0.530	2.067
2	0.65	0.490	0.926
3	0.70	0.511	0.570
4	0.73	0.507	0.957
5	0.59	0.333	0.783
6	0.73	0.527	1.937
7	0.74	0.512	1.749
8	0.54	0.618	2.923
9	0.52	0.573	2.449
10	0.56	0.724	0.773
11	0.72	0.517	2.220
12	0.71	0.506	0.708
13	0.74	0.506	0.837
14	0.70	0.552	2.175
15	0.73	0.528	1.925
16	0.70	0.552	2.143
17	0.73	0.529	1.795
18	0.73	0.525	1.773

where δd is the energy from dispersion forces, δp represents the energy from dipolar intermolecular forces and δh is the energy from hydrogen bonds between molecules. d , p , and h are regression coefficients that show the extent of interactions represented (Hansen 2007). Table 6 shows the results obtained.

Based on the numerical values of the regression coefficients in Table 6, where regression coefficient d has the highest value, it can be concluded that the most dominant forces between tested carbohydrazones and the solvent used are the dispersion forces. They are followed by the possibility of building hydrogen bonds (regression coefficient h), and finally, with a very small effect, dipolar forces are represented (regression coefficient p). Results obtained by correlation with Hansen's solubility parameters are in agreement with the results obtained by the application of the Kamlet–Taft's model, and it can be concluded that nonspecific interactions are more dominant and have a greater influence on maxima shifting of the monocarbohydrazone derivatives than the specific ones.

The influence of the substituent on the absorption spectra of carbohydrazones

In addition to the medium in which the substance is dissolved, the appearance of absorption spectra is also influenced by the structure of the molecule, i.e., the distribution of electron density. In the case of the investigated carbohydrazones, the appearance of the spectrum depends on the type and position

of the substituent present on the benzene ring. Quantitative analysis of this impact is given by applying the linear free energy relationship (LFER) to Hammett's equation:

$$\nu_{\max} = \nu_0 + \rho\sigma_{m,p}, \quad (4)$$

where ν_{\max} is absorption frequency at the maximum of absorbance, ν_0 represents the wave number in the irrespective solvent, ρ is a proportionality constant reflecting the sensitivity of the spectral data to the substituent effects, described by the substituent constant, $\sigma_{m,p}$ (Hammett's constant) (Hammett 1937).

In Fig. 4, spectra of all compounds recorded in methanol are represented. Since Hammett's equation does not give a description for the substituents in the ortho position, compounds 2, 5, 8 and 11 are left out from the correlations.

As can be seen, most of the compounds tested give smaller or bigger bathochromic shifts relative to the unsubstituted compound, 1 (4-H). The exceptions are compounds 2, 8, 11 and 18 where hypsochromic shifts were noticed. The numerical values of the Hammett's constants of substituents are given in Table 7.

Correlating these constants to the absorption maxima of the compounds tested, linear dependencies are obtained, such as the dependence in Fig. 5.

Two separate linear dependences were obtained. The first, dependence with the positive slope, represents electron-donor substituents, while the other is for substituents with electron-acceptor properties (negative slope), with the deviation for compound 9 (3-NO₂). Coefficients of the obtained linear correlations are presented in Table 8.

The absolute value of the proportionality constant, ρ , determines the extent of substituent's influence on the change of electronic density in the molecule. A positive sign of the proportionality constants in all solvents in the case where substituents are electron donors indicates an increased electron density in the excited state in relation to the basic. When substituents of the tested derivatives have an electron-acceptor's nature, the proportionality constant has a negative value, which indicates a reduced electron density in the excited state. Based on the results obtained in Table 8, it can be concluded that the electron-acceptor's substituents have a greater influence on the spectral properties of the compounds tested due to the higher value of the proportionality constant, ρ . On the other hand, properties of the solvents used have no significant effect on the absorption changes caused by the nature of the substituent. (Values of the proportionality constants for all solvents used are very close).

Computational results

Photon absorption can induce a deformation in the molecular electronic cloud and can cause a partial shift of electrons

from one part of the molecule to another, known as intramolecular charge transfer (ICT). An efficient way to estimate a character of excitation is by calculating Tozer's Λ diagnostic index. The Λ index represents the spatial overlap between the occupied and virtual orbitals involved in the selected excitation and can have a value between 0 and 1, with 1 indicating a perfect overlap between orbitals (no intermolecular charge transfer) and value of 0 indicating complete separation of occupied and virtual orbitals. Based on extensive benchmark calculations (Peach et al. 2008; Peach et al. 2009; Peach and Tozer 2009), values of $\Lambda > 0.3$ represent localized, short-range transition.

Results of the calculations of Λ index and ICT indices, charge-transfer distance (D_{CT}) and amount of transferred charge (Q_{CT}), for *Z* isomers of all investigated compounds, are shown in Table 9. All investigated compounds, except compounds with nitro substituent (compounds 8–10), have large Λ values, indicating a small amount of ICT between the ground and the excited states. This is confirmed by calculations of the amount of transferred charge (Q_{CT}) index which is in the range between $0.333 e^-$ and $0.552 e^-$. Transitions in compounds with a nitro group (compounds 8–10) show somewhat more pronounced ICT character; Λ values between 0.52 and 0.56 and Q_{CT} values between $0.573 e^-$ and $0.724 e^-$ (Table 9).

In Fig. 6, the difference between electronic densities in the ground and excited states (top part) and positions of charge loss and charge gain barycenters (bottom part) are shown. For example, in the unsubstituted compound, during excitation, there is a charge transfer of $0.530 e^-$ from phenyl group to the carbonyl moiety with charge-transfer distance (D_{CT}) at 2.067 \AA . The similar ICT process is observed in compounds 6, 7, 9, 11 and 14–18 (D_{CT} values between 1.773 \AA and 2.449 \AA). In compound 8, the larger amount of charge ($0.618 e^-$) is transferred across the longer distance (2.293 \AA) from the nitro group in the ortho position to the carbonyl part of the molecule. In other compounds, no significant ICT processes can be observed due to short D_{CT} values (Table 9, Fig. 6).

In order to further support experimental findings and confirmation of $n \rightarrow \pi^*$ nature of first transition state, TD-DFT calculations with B3LYP/6-311G(*d,p*) method of *Z* and *E* isomers of all synthesized molecules were performed. The calculations were done in two different solvents: methanol (polar protic) and DMSO (polar aprotic). For comparison purposes, Fig. 7 shows the experimental and theoretical UV spectra of compound 17, both in DMSO and in methanol as a solvent. The summary of the calculation results is presented in Tables S3–S6.

Due to the large values of Λ index (Table 9), we expected a hybrid functional to perform well (Peach et al. 2008; Peach et al. 2009), and, in general, there is a reasonably good

agreement between calculated and experimentally observed results. Most of the compounds have bathochromic shifts relative to the unsubstituted compound except compound 8. Also, compound 2 in its most stable *E* isomer form shows a significant hypsochromic shift (around 17 nm) in both solvents due to the formation of a strong intramolecular hydrogen bond. In the *Z* isomer of compound 2, no intramolecular hydrogen bond can be formed due to steric constraints, and, as expected, there is a bathochromic shift when compared to compound 1. Also, TD-DFT calculations were able to correctly predict the hypsochromic shift in methanol, when compared to DMSO, for both isomers of all investigated compounds, and this is in line with experimentally observed results.

TD-DFT calculations have shown that, due to its planar geometries, *E* isomers have first absorption maxima at lower energies than *Z* isomers. Again, compound 2 is the exception; the first absorption maximum for *E* isomer is 13.49 and 13.90 nm lower in DMSO and methanol than for the *Z* isomer (Tables S3–S6).

From Tables S3–S6, it can be seen that in *Z* and *E* isomers of almost all investigated compounds [except 2 (*E* form), 8 and 9 (*Z* form)] the main contribution to the first excited state comes from HOMO–LUMO single-particle excitation. In order to visualize the nature of this excitation, the orbitals with the highest contribution were localized using the NBO localization procedure and are shown in Fig. 8 for the most stable isomer of every investigated compound. All the HOMO orbitals (HOMO-1 for compound 2, *E* form) are nonbonding in nature, mainly acting as electron pair on the oxygen atom. All the LUMO orbitals (LUMO + 1 for compounds 8 and 9 (*Z* form)) are π anti-bonding in nature. This is in agreement with our previous statement that $n \rightarrow \pi^*$ transitions are responsible for the first absorption maxima.

Conclusion

Eighteen monocarbonylhydrazones were synthesized and characterized using different methods. The purity of the compounds made was confirmed using NMR ^{13}C , ^1H , IR and elemental analysis. Giving the fact that the presence of imino group allows *E/Z* isomerization, some of the synthesized compounds were presented as a mixture of both isomers and their stereochemistry was established using 2D NMR techniques. Obtained results showed that *E* form dominates in DMSO solution.

UV spectra of the tested derivatives were recorded in the range from 200 to 400 nm in nineteen solvents of different properties. It was assumed and confirmed that the analyzed maxima came as a result of $n \rightarrow \pi^*$ transition in molecules.

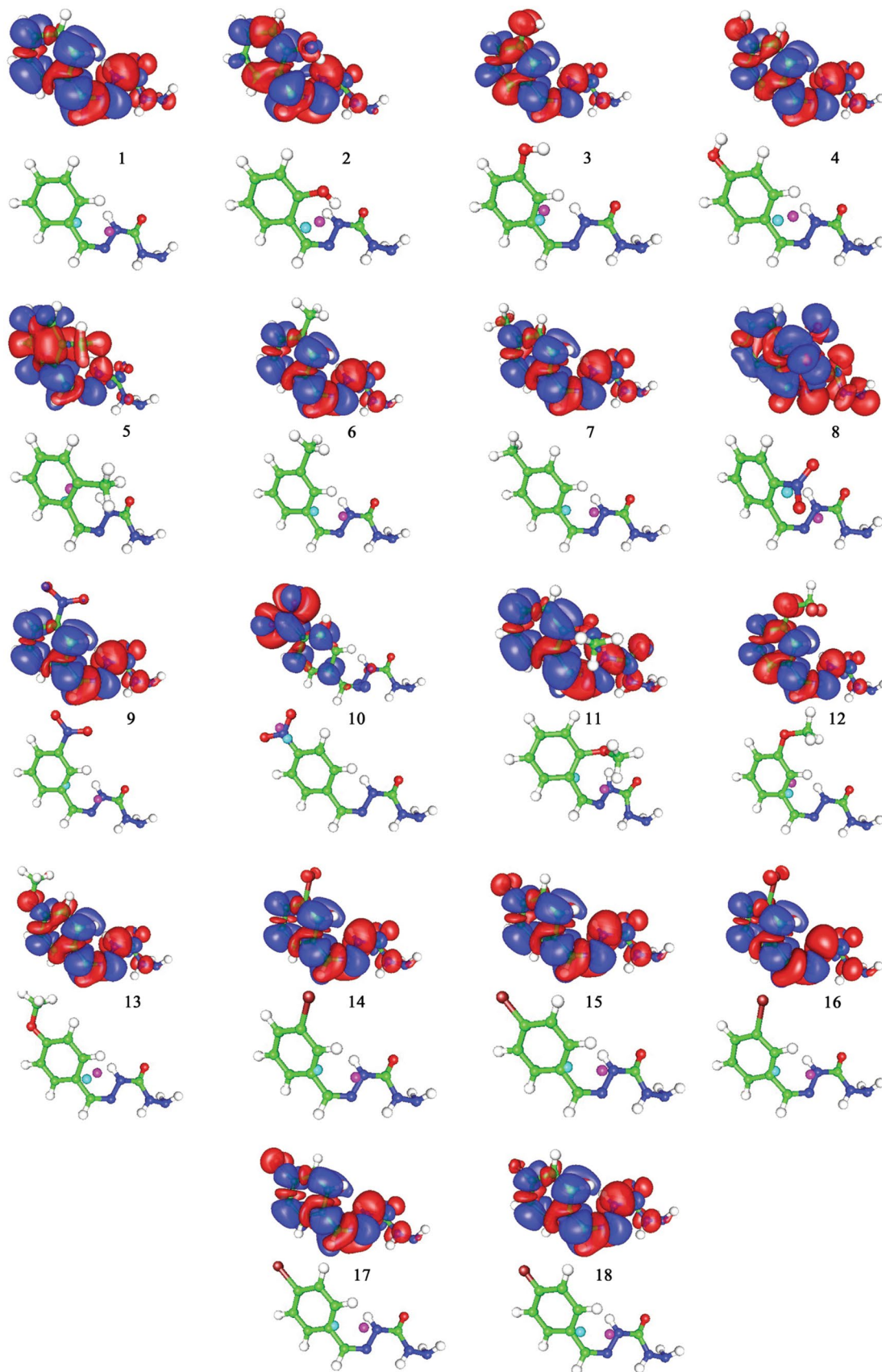


Fig. 6 ICT processes in *Z* isomers of compounds 1–18, top images—difference between densities in excited and ground states (red and blue—density increase and decrease upon transition, respectively); bottom images—positions of barycenters for charge loss (cyan circle) and charge gain (violet circle) upon transition

The effects of specific and nonspecific interactions on the UV absorption maxima shifts of the monocarbohydrazones were studied using two models, Kamlet–Taft's and Catalan's. In addition to this, correlations of the absorption maxima with Hansen's solubility parameters were made in order to obtain additional information about the interactions that occur between the investigated compounds and the surrounding medium. Results obtained by correlating different empirical parameters of the solvents used with absorption frequencies of the compounds tested show that nonspecific interactions (polarizability and dipolarity) are more dominant and have a greater influence on maxima shifting of the monocarbohydrazones. Slightly smaller influence has acidity, while the smallest influence has the basicity of the surrounding medium.

The influence of the structure on the absorption maxima shifts was interpreted using Hammett's equation. Two dependencies were obtained, one for electron-donor substituents and one for electron-acceptor substituents. Based on the results obtained, electron-acceptor substituents have a greater influence on the spectral properties of the compounds tested due to the higher value of the proportionality constant, ρ .

Energies obtained from ab initio calculations at MP2/6-311G(*d,p*) level of theory have shown that *Z* isomer is 2.38–5.84 kcal/mol more stable for all compounds, except for compound 2 where *E* configuration shows higher stability due to the formation of the intermolecular hydrogen bond.

In order to further support experimental findings and confirmation of $n \rightarrow \pi^*$ nature of first transition state, TD-DFT calculations with B3LYP/6-311G(*d,p*) calculations of *Z* and *E* isomers of all synthesized molecules were performed in two different solvents: methanol (polar protic) and DMSO (polar aprotic). In general, there was a reasonably good agreement between calculated and experimentally observed results. Most of the compounds had a bathochromic shift relative to the unsubstituted compound. Also, TD-DFT calculations were able to correctly predict the hypsochromic shift in methanol, when compared to DMSO, for both isomers of all investigated compounds, and this is in line with experimentally observed results.

In *Z* and *E* isomers of almost all investigated compounds, the main contribution to the first excited state came from HOMO–LUMO single particle excitation. All the HOMO orbitals are nonbonding in nature, mainly acting as electron pair on the oxygen atom. All the LUMO orbitals are π anti-bonding in nature. This is in agreement with our previous statement that $n \rightarrow \pi^*$ transitions are responsible for the first absorption maxima.

Results of the calculations of ICT indices, charge-transfer distance (D_{CT}) and amount of transferred charge (Q_{CT}), for *Z* isomers of all investigated compounds showed that in the unsubstituted compound, during excitation, there was a charge transfer of $0.530 e^-$ from phenyl group to the carbohydrazide moiety. A similar ICT process was observed in compounds 6, 7, 9, 11 and 14–18. In compound 8, the larger amount of charge ($0.618 e^-$) is transferred across the longer distance (2.293 Å) from the nitro group in the ortho position to the carbohydrazide part of the molecule. In other compounds, no significant ICT processes could not be observed due to short D_{CT} values.

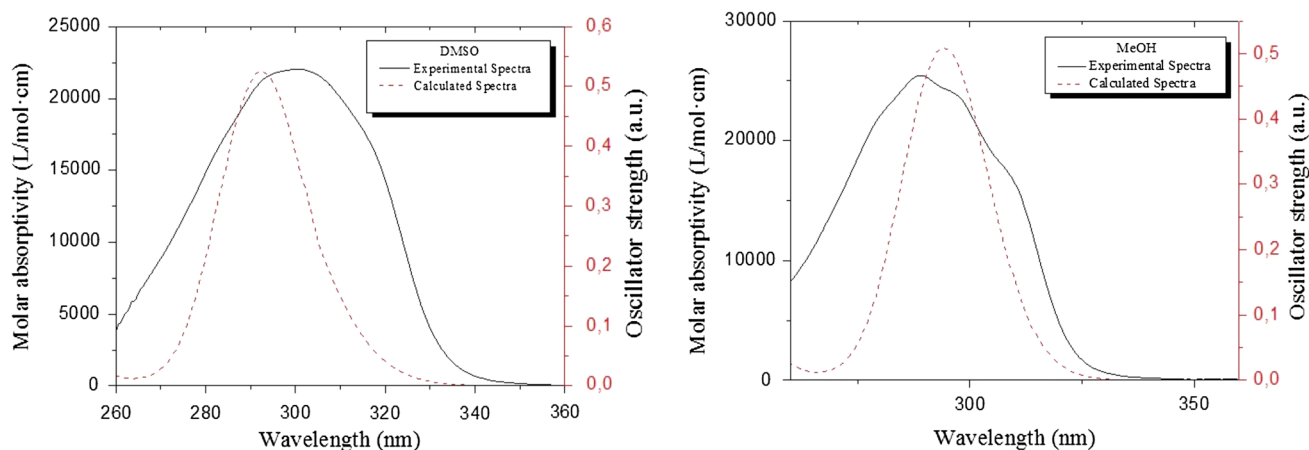


Fig. 7 Experimental and theoretical UV spectra of compound 17 in DMSO and methanol

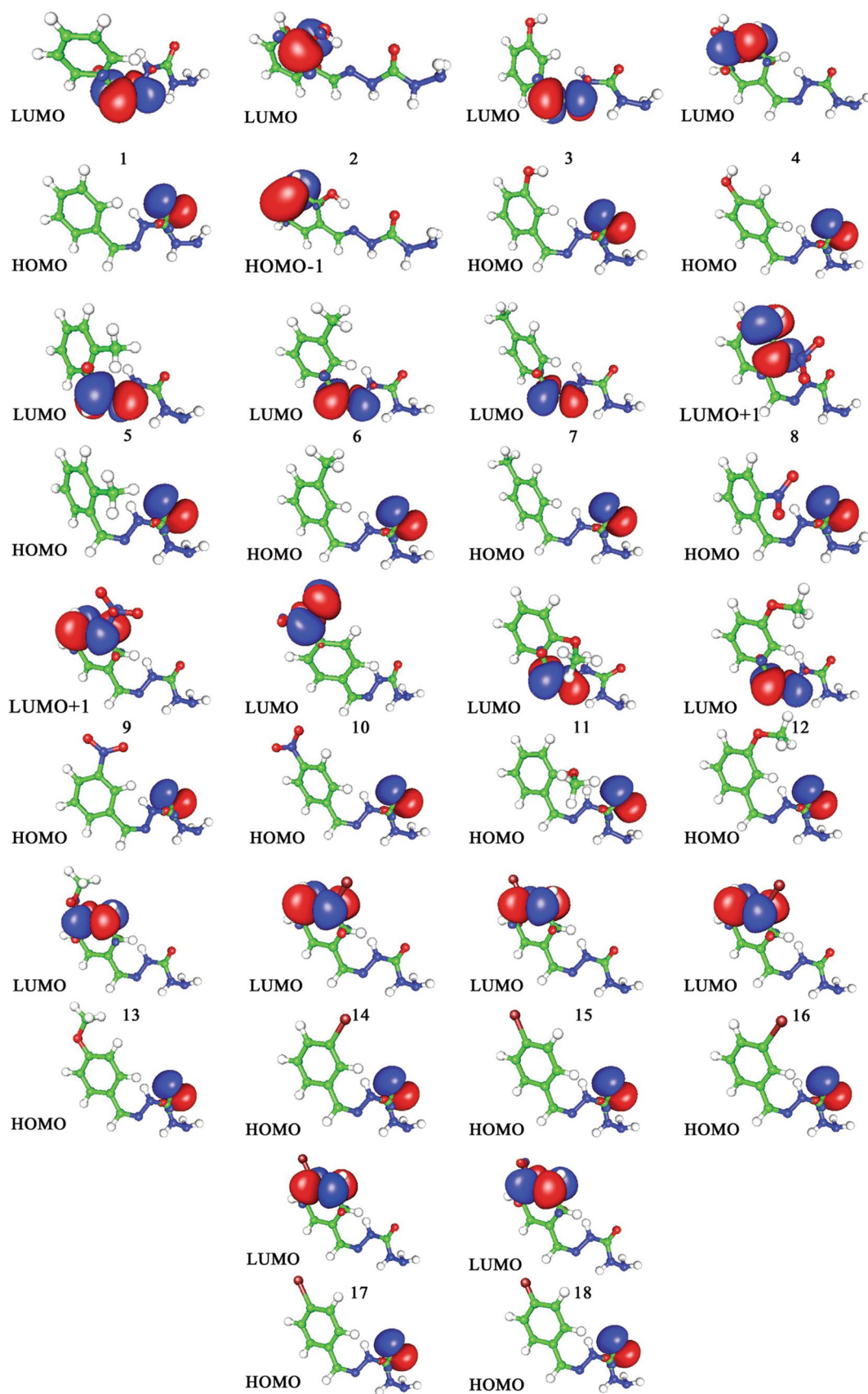


Fig. 8 Frontier orbitals with the highest CI expansion coefficients, localized by NBO localization procedure for the most stable isomers of all investigated compounds

Acknowledgements This work was supported by the Ministry of Education, Science and Technological Development of the Republic of Serbia (Project 172013).

Compliance with ethical standards

Conflict of interest The authors declare that they have no conflict of interest.

References

- Antić-Jovanović A (2006) Molekulska spektroskopija-spektrohemijski aspekti, fakultet za fizičku hemiju, Beograd
- Babahan I, Anil H, Sarikavakli N (2011) Synthesis of novel tetraoxime derivative with hydrazone side groups and its metal complexes. *Turk J Chem* 35:613–624. <https://doi.org/10.3906/kim-1003-105>
- Bacchi A, Carcelli M, Pelagatti P, Pelizzi C, Pelizzi G, Zani F (1999) Antimicrobial and mutagenicity of some carbon- and thio-carbonohydrazone ligands and their copper(II), iron(II) and zinc(II) complexes. *J Inorg Biochem* 75:123–133. [https://doi.org/10.1016/S0162-0134\(99\)00045-8](https://doi.org/10.1016/S0162-0134(99)00045-8)
- Bauer M, Rollberg A, Barth A, Spange S (2008) Differentiating between dipolarity and polarizability effects of solvents using the solvatochromism of barbiturate dyes. *Eur J Org Chem* 2008:4475–4481. <https://doi.org/10.1002/ejoc.200800355>
- Becke AD (1993) A new mixing of Hartree–Fock and local density-functional theories. *J Chem Phys* 98:1372–1377. <https://doi.org/10.1063/1.464304>
- Božić AR, Filipović NR, Novaković IT, Bjelogrić SK, Nikolić JB, Drmanić SŽ, Marinković AD (2017) Synthesis, antioxidant and antimicrobial activity of carbohydrazones. *J Serb Chem Soc* 82:495–508. <https://doi.org/10.2298/JSC161220045B>
- Božić A, Marinković A, Bjelogrić S, Todorović TR, Cvijetić IN, Novaković I, Müller CD, Filipović NR (2016) Quinoline based mono- and bis-(thio)carbohydrazones: synthesis, anticancer activity in 2D and 3D cancer and cancer stem cell models. *RSC Adv* 6:104763–104781. <https://doi.org/10.1039/c6ra23940d>
- Božić AR, Filipović NR, Verbić TŽ, Milčić MK, Todorović TR, Cvijetić IN, Klisurić OR, Radišić M, Marinković AD (2017) A detailed experimental and computational study of monocarbohydrazones. *Arab J Chem*. <https://doi.org/10.1016/j.arabj.c.2017.08.010>
- Catalán J (2009) Toward a generalized treatment of the solvent effect based on four empirical scales: dipolarity (SdP, a new scale), polarizability (SP), acidity (SA), and basicity (SB) of the medium. *J Phys Chem B* 113:5951–5960. <https://doi.org/10.1021/jp809572f>
- Catalán J, Hopf H (2004) Empirical treatment of the inductive and dispersive components of solute-solvent interactions: the solvent polarizability (SP) scale. *Eur J Org Chem* 2004:4694–4702. <https://doi.org/10.1002/ejoc.200400311>
- Dragancea D, Talmaci N, Shova S, Novitchi G, Darvasiova D, Raptă P, Breza M, Galanski M, Kožiček J, Martins NMR, Martins LMDRS, Pombeiro AJL, Arion VB (2016) Vanadium(V) complexes with substituted 1,5-bis(2-hydroxybenzaldehyde) carbohydrazones and their use as catalyst precursors in oxidation of cyclohexane. *Inorg Chem* 55:9187–9203. <https://doi.org/10.1021/acs.inorgchem.6b01011>
- Frisch MJ, Trucks GW, Schlegel HB, Scuseria GE, Robb MA, Cheeseman JR, Scalmani G, Barone V, Petersson GA, Nakatsuji H, Li X, Caricato M, Marenich AV, Bloino J, Janesko BG, Gomperts R, Mennucci B, Hratchian HP, Ortiz JV, Izmaylov AF, Sonnenberg JL, Williams-Young D, Ding F, Lipparini F, Egidi F, Goings J, Peng B, Petrone A, Henderson T, Ranasinghe D, Zakrzewski VG, Gao J, Rega N, Zheng G, Liang W, Hada M, Ehara M, Toyota K, Fukuda R, Hasegawa J, Ishida M, Nakajima T, Honda Y, Kitao O, Nakai H, Vreven T, Throssell K, Montgomery JA, Peralta JE, Ogliaro F, Bearpark MJ, Heyd JJ, Brothers EN, Kudin KN, Staroverov VN, Keith TA, Kobayashi R, Normand J, Raghavachari K, Rendell AP, Burant JC, Iyengar SS, Tomasi J, Cossi M, Millam JM, Klene M, Adamo C, Cammi R, Ochterski JW, Martin RL, Morokuma K, Farkas O, Foresman JB, Fox DJ (2016) Gaussian 16, Revision B.01, Gaussian, Inc., Wallingford CT
- Gangarapu K, Manda S, Jallapally A, Thota S, Karki SS, Balzarini J, De Clercq E, Tokuda H (2014) Synthesis of thiocarbohydrazone and carbohydrazone derivatives as possible biologically active agents. *Med Chem Res* 23:1046–1056. <https://doi.org/10.1007/s00044-013-0684-3>
- Gholivand K, Farshadfar K, Roe SM, Gholami A, Esrafil MD (2016) Structural and photophysical characterization of mono- and binuclear Cu(I) complexes based on carbohydrazones: a combined experimental and computational study. *CrystEngComm* 18:2873–2884. <https://doi.org/10.1039/c5ce02208h>
- Glendening ED, Reed AE, Carpenter JE, Weinhold F (2003) NBO Version 3.1. Gaussian Inc., Pittsburgh
- Hammett P (1937) The effect of structure upon the reactions of organic compounds. Benzene derivatives. *J Am Chem Soc* 59:96–103. <https://doi.org/10.1021/ja01280a022>
- Hansen ChM (2007) Solubility parameters: a user's handbook. CRC Press-Taylor & Francis group, Boca Raton
- Iqbal S, Saleem M, Azim MK, Taha M, Salar U, Khan KM, Perveen S, Choudhary MI (2017) Carbohydrazones as new class of carbonic anhydrase inhibitors: synthesis, kinetics and ligand docking studies. *Bioorg Chem* 72:89–101. <https://doi.org/10.1016/j.bioorg.2017.03.014>
- Jacquemin D, Le Bahers T, Adamo C, Ciofini I (2012) What is the “best” atomic charge model to describe through-space charge-transfer excitations? *Phys Chem Chem Phys* 14:5383–5388. <https://doi.org/10.1039/C2CP40261K>
- Kajal A, Bala S, Sharma N, Kamboj S, Saini V (2014) Therapeutic potential of hydrazones as anti-inflammatory agents. *Int J Med Chem*. <https://doi.org/10.1155/2014/761030>
- Kamlet MJ, Taft RW (1976) The solvatochromic comparison method. I. The β -scale of solvent hydrogen-bond acceptor (HBA) basicities. *J Am Chem Soc* 98:377–383. <https://doi.org/10.1021/ja00418a009>
- Kamlet MJ, Abboud JLM, Taft RW (1977) The solvatochromic comparison method. 6. The π scale of solvent polarities. *J Am Chem Soc* 99:6027–6038. <https://doi.org/10.1021/ja00460a031>
- Kamyabi MA, Soleymani-Bonoti F, Bikas R, Hosseini-Monfared H (2017) Oxygen reduction catalyzed by a carbohydrazone based compound at liquid/liquid interfaces. *J Electroanal Chem* 794:235–243. <https://doi.org/10.1016/j.jelechem.2017.04.021>
- Kurzer F, Wilkinson M (1970) Chemistry of carbohydrazone and thiocarbohydrazone. *Chem Rev* 70:111–149. <https://doi.org/10.1021/cr60263a004>
- Le Bahers T, Adamo C, Ciofini I (2011) A qualitative index of spatial extent in charge-transfer excitations. *J Chem Theory Comput* 7:2498–2506. <https://doi.org/10.1021/ct200308m>
- Montazerzohori M, Yadegari S, Naghiha A (2014) Synthesis, characterization, electrochemical behavior and antibacterial/antifungal activities of [Cd(L)X₂] complexes with a new Schiff base ligand. *J Serb Chem Soc* 79:793–804. <https://doi.org/10.2298/JSC130520110M>

- Okawara T, Imai K, Ochiai T (2006) Free radical scavenger containing semicarbazide derivatives. WO 2006093124
- Peach MJG, Tozer DJ (2009) Illustration of a TDDFT spatial overlap diagnostic by basis function exponent scaling. *J Mol Struct Theochem* 914:110–114. <https://doi.org/10.1016/j.theochem.2009.03.009>
- Peach MJG, Benfield P, Helgaker T, Tozer DJ (2008) Excitation energies in density functional theory: an evaluation and a diagnostic test. *J Chem Phys* 128:044118. <https://doi.org/10.1063/1.2831900>
- Peach MJG, Le Sueur CR, Ruud K, Guillaume M, Tozer DJ (2009) TDDFT diagnostic testing and functional assessment for triazene chromophores. *Phys Chem Chem Phys* 11:4465–4470. <https://doi.org/10.1039/b822941d>
- Reed AE, Weinhold F (1985) Natural localized molecular orbitals. *J Chem Phys* 83:1736–1740. <https://doi.org/10.1063/1.449360>
- Reichardt Ch (2003) Solvents and solvent effects in organic chemistry, 3rd edn. Wiley-VCH, Weinheim
- Riedel F, Spange S (2012) Solvatochromism of catechol derivatives—solute/solvent interactions. *J Phys Org Chem* 25:1261–1268. <https://doi.org/10.1002/poc.3003>
- Rollas S, Küçükgüzel SG (2007) Biological activities of hydrazone derivatives. *Molecules* 12:1910–1939. <https://doi.org/10.3390/12081910>
- Sánchez Rojas F, Cristófol Alcaraz E, Cano Pavón JM (1994) Determination of aluminium in water by flow injection with fluorimetric detection by using salicylaldehydecabo-hydrazone as reagent in a micellar medium. *Analyst* 119:1221–1223. <https://doi.org/10.1039/AN9941901221>
- Shebl M, Khalil SME (2015) Synthesis, spectral, X-ray diffraction, antimicrobial studies and DNA binding properties of binary and ternary complexes of pentadentate N₂O₃ carbohydrazone ligands. *Monatsh Chem* 146:15–33. [10.1007/s00706-014-1302-x](https://doi.org/10.1007/s00706-014-1302-x)
- Taft RW, Kamlet MJ (1976) The solvatochromic comparison method. 2. The α -scale of solvent hydrogen-bond donor (HBD) acidities. *J Am Chem Soc* 98:2886–2894. <https://doi.org/10.1021/ja00426a036>
- Wang LH, Liang L, Li PF (2017) Synthesis, crystal structure, catalytic properties, and luminescent of a novel Eu(III) complex material with 4-Imidazolecarboxaldehyde-pyridine-2-carbohydrazone. *Bull Chem React Eng Catal* 12:185–190. <https://doi.org/10.9767/bcrec.12.2.764.185-190>
- Warkentin J, Ramakrishnan K, Jain RC, Wandelmaier FW (1977) Oxadiazoline derivatives. US424272000
- Wiggins P, Williams JAG, Tozer DJ (2009) Excited state surfaces in density functional theory: a new twist on an old problem. *J Chem Phys*. <https://doi.org/10.1063/1.3222641>
- Yanai T, Tew DP, Handy NC (2004) A new hybrid exchange-correlation functional using the Coulomb-attenuating method (CAM-B3LYP). *Chem. Phys Lett* 393:51–57. <https://doi.org/10.1016/j.cplett.2004.06.011>
- Zelenin KN, Alekseev VV, Kuznetsova OB, Saminskaya AG, Yakimovich SI, Zverova IV (1999) Carbohydrazones and their ring-chain tautomerism. *Russ J Org Chem* 35:357–363
- Zhang J, Zhang T, Yu K (2006) The preparation, molecular structure and theoretical study of carbohydrazone (CHZ). *Struct Chem* 17:249–254. <https://doi.org/10.1007/s11224-006-9015-3>

Publisher's Note Springer Nature remains neutral with regard to jurisdictional claims in published maps and institutional affiliations.